Preparation and characteristics of glass foam

Østergaard, Martin Bonderup

DOI (link to publication from Publisher):
10.5278/vbn.phd.eng.00073

Publication date:
2019

Document Version
Publisher's PDF, also known as Version of record

PREPARATION AND CHARACTERISTICS OF GLASS FOAM

BY
MARTIN BONDERUP ØSTERGAARD

DISSERTATION SUBMITTED 2019

AALBORG UNIVERSITY
DENMARK

PhD Dissertation

Preparation and characteristics of glass foam

by

Martin Bonderup Østergaard

Section of Chemistry

Department of Chemistry and Bioscience

Aalborg University, Denmark

AALBORG UNIVERSITY
DENMARK

Dissertation submitted 2019

Date of Defence

April 5th 2019

Dissertation submitted: January 2019

PhD supervisor: Professor Yuanzheng Yue
Aalborg University, Denmark

PhD committee: Associate Professor Rasmus Lund Jensen (chairman)
Aalborg University

Professor Paolo Colombo
University of Padova

Dr. Manoj K. Choudhary
Senior Advisor for Strategic Affairs
Glass Servuce, Inc., USA

PhD Series: Faculty of Engineering and Science, Aalborg University

Department: Department of Chemistry and Bioscience

ISSN (online): 2446-1636
ISBN (online): 978-87-7210-382-2

Published by:
Aalborg University Press
Langagervej 2
DK – 9220 Aalborg Ø
Phone: +45 99407140
aauf@forlag.aau.dk
forlag.aau.dk

Printed in Denmark by Rosendahls, 2019

ENGLISH SUMMARY

Glass foams are attractive materials that can be used for different applications such as lightweight fillings and thermal or sound insulation. As thermal insulator, the thermal conductivity is a crucial property that should be kept as low as possible without compromising other properties. However, the understanding of thermal conductivity of glass foams is still limited due to lack of reported data. Therefore, the aim of this PhD project was to enhance the understanding by investigating the effects of solid and gas phases and porous structure on the thermal conductivity of glass foams. We prepared glass foams from obsolete cathode ray tube (CRT) panel glasses throughout the present thesis as it has a low thermal conductivity compared to other waste silicate glasses such as flat glass and bottle glass, and large amounts of CRT glass is landfilled, and thus, being harmful to our environment.

First, we studied the foaming of a common CRT panel glass, Mn_3O_4, and carbon mixture while adding different alkali (Li, Na, K) phosphates to the mixture. Various types of sodium phosphates are claimed to have a foam stabilizing effect, however, this is not proved in literature. We found no effect of the alkali phosphates on pore size, pore shape, or wall thickness. However, we showed that K_3PO_4 is promising to obtain closed pores of highly porous glass foams.

Second, we investigated the effect of pressure and gas specie on the foaming behavior using a physical foaming approach. Glass powder was sintered under high pressure of inert gases (He, Ar, N_2) which resulted in a pellet with high gas pressure in closed pores. Subsequent reheating of the pellet caused expansion due to the combination of decreasing viscosity of the glass and the release of the high gas pressure. We found that the kinetic diameter of the gas species greatly affected the foaming onset, maximum expansion, and thus, the final foam characteristics. On the contrary, the pressure dependence showed an optimum pressure of 20 MPa.

Third, we studied the effect of solid phase, gas phase, and macrostructure on the thermal conductivity of glass foams. In order to optimize the insulating ability of glass foams, it is necessary to enhance the knowledge of the contribution of different phases and structure to the thermal conductivity of glass foams. We found that the thermal conductivity of the solid phase increases with increasing content of foaming agent dissolved in the glass structure. Moreover, the thermal conductivity increases with increasing crystal content in the samples. The gas phase contribution to thermal conductivity of glass foams was investigated by entrapping Ar or N_2 by physical foaming, however, CO_2 was present giving binary gas mixtures. Theoretical calculations of the thermal conductivity of gas mixtures proved that the Ar-rich gas phases had a lower thermal conductivity than that of the N_2-rich ones resulting in a lower thermal conductivity of the glass foams. Finally, we found that an increase in average pore size from 0.10–0.16 mm decreases the thermal conductivity by >10 %.

DANSK RESUME

Glasskum er et attraktivt materiale, der kan bruges til forskellige formål såsom letvægtsfyld i vejkonstruktioner og varme- eller lydisolering. Som varmeisolering er varmeledningsevnen en afgørende egenskab, der skal gøres så lav som muligt uden at gå på kompromis med andre egenskaber. Forståelsen af varmeledningsevnen af glasskum er dog begrænset på grund af mangel på data. Derfor er målet med dette PhD-projekt at øge forståelsen af varmeledningsevnen af glasskum ved at undersøge effekten af den faste fase og gasfasen samt den porøse struktur. I denne afhandling har vi lavet glasskum fra forældede frontglas fra billedrør (CRT-glas), da det har en lav varmeledningsevne sammenlignet med andre restglas som f.eks. vinduesglas og flaskeglas. Derudover bliver store mænger billedrør deponeret på lossepladser, hvilket er skadeligt for miljøet.

Vi har studeret skumningen af en almindelig skumglasblanding bestående af CRT-glas, Mn_3O_4 og kul, hvor vi tilsatte forskellige alkalifosfater (Li, Na, K). Forskellige typer af natriumfosfater påstås at have en skumstabiliserende effekt, men dette er ikke bevist. Vi fandt ingen effekt af alkalifosfaterne på porestørrelse, poreform eller vægtykkelse af skumglassene. Dog viste K_3PO_4 lovende resultater i forhold til at opnå lukkede porer for højporøse glasskum.

Derudover undersøgte vi effekten af tryk og gasart på skumningsadfæren, når vi bruger en fysisk skumningstilgang. Glaspulver blev sintret under højt tryk ved at bruge inerte gasser (He, Ar, N_2), hvilket resulterede i en pille med et højt gastryk i lukkede porer. Efterfølgende opvarmning af denne pille medførte udvidelse som følge af det høje tryk og den kontinuert faldende viskositet af glasset. Vi fandt, at den kinetiske diameter af gasarten havde stor indflydelse på, hvornår skummningen startede, den maksimale udvidelse og dermed de endelige karakteristika af glasskummet. Derudover påviste vi, at der er et optimalt tryk på 20 MPa under sintring i forhold til at opnå en maksimal skumning og dermed en høj porøsitet.

Desuden har vi undersøgt effekten af fastfasen, gasfasen og makrostrukturen på varmeledningsevnen af glasskum. For at kunne optimere isoleringsevnen af glasskum er det nødvendigt at opnå viden om, hvordan disse faser bidrager til den samlede varmeledningsevne af glasskum. Vi påviste, at varmeledningsevnen af den faste fase stiger, når indholdet af skumningsagenter stiger og ligeledes, når krystalindholdet i glasfasen øges. Gasfasens bidrag blev undersøgt ved at fange Ar og N_2 i gasfasen ved fysisk skumning, dog blandet med CO_2, hvilket skabte binære gasblandinger. Teoretiske beregninger viste, at de Ar-rige gasfaser havde en lavere varmeledningsevne end de N_2-rige, hvilket resulterede i en lavere varmeledningsevne af glasskummene med Ar i gasfasen. Slutteligt fandt vi ud af, at varmeledningsevnen faldt >10 %, når den gennemsnitlige porestørrelse blev øget fra 0.10-0.16 mm.

ACKNOWLEDGEMENTS

This thesis has been submitted for assessment in partial fulfillment of the PhD degree. The thesis is based on published (and submitted) scientific papers listed in Section 1.3. The work was conducted at Section of Chemistry at Aalborg University from October 2015 to January 2019. This study is part of an interdisciplinary CleanTechBlock II project financed by the The Energy Technology Development and Demonstration Program (EUDP). It is a collaboration between Section of Chemistry and Department of Civil Engineering (Aalborg University, AAU), Department of Advanced Materials (Jožef Stefan Institute, JSI), and Gråsten Brickwork A/S.

First of all, I wish to thank my supervisor YuanzhengYue for his guidance and inspiration throughout this PhD project. I have enjoyed our discussions and collaboration, and I appreciate that you always find the time to discuss new studies, results, and drafts.

I want to thank Rasmus R. Petersen (AAU) and Jakob König (JSI) for countless discussions about new studies, foaming processes, thermal conductivity, and various results. It has been a great pleasure to collaborate with you both.

My kind acknowledgement go to Jacob Bendtsen from Gråsten Brickwork for a pleasant cooperation and providing the glass powder. Special thanks go to external collaborators from different studies. Thanks to Hicham Johra (AAU) for his kind guidance in the Laser Flash technique. Thanks to Michal Bockowski (Polish Academy of Sciences) for high pressure sintering of samples. Thanks to the whole Manchester University X-Ray Imaging Facility group at Research Complex at Harwell (RCaH), especially Professor Peter D. Lee (now at University College London) and Biao Cai (now at Birmingham University) for discussions and their guidance in 3D imaging. In relation to the external stay at RCaH, I appreciate the external funding by *Oticon Fonden* and *IDAs og Berg-Nielsens Studie- og støttefond*

Thanks to present and former members of the Section of Chemistry at Aalborg University for providing a pleasant working environment and countless discussions. I have enjoyed every work and non-work related discussion with you. A special thanks to the “lunch club” for always giving a pleasant midday break.

A special thanks go to my family. Thanks to my parents Helle and Henning for always believing in me and supporting me whenever needed. Thanks to my brother Mads for your support.

Finally, a very special thanks to my wife Anette for being patient, understanding, supporting, and always believing in me, and to my son Lucas for great smiles and laughs.

TABLE OF CONTENTS

CHAPTER 1. INTRODUCTION

Insulation materials have always been of great interest to mankind and society starting with clothes to keep the body warm and later to build and insulate houses. Nowadays, the insulation standard of houses is improving in order to reduce the energy consumption on heating up the houses. One way to improve the insulation is to increase the thickness of the insulating material which is observed for both walls and roofs in many European countries [1]. This is a consequence of the lack of improvement of the insulating ability of various insulation materials. Unfortunately the increasing insulation thickness leads to a reduced living-to-house area ratio, and thus, it is getting more expensive to maintain the same living area in Denmark as the tax is calculated from the house area. Therefore, improvement of current or development of new insulation materials is of great interest.

Among the traditional insulation materials for buildings are mineral wool, expanded polystyrene (EPS), extruded polystyrene (XPS), and polyurethane (PUR), while recent state-of-the-art insulation materials cover vacuum insulation panels (VIPs), gas-filled panels (GFPs), and aerogels [2]. Most of the primary used insulation materials are organic except of mineral wool that are inorganic [3]. Another inorganic insulation material is glass foam which is not among the traditional materials but shows good properties. As insulation material the thermal conductivity is a crucial property as it defined as the rate of heat to transfer through a material. Therefore, a good insulation material has a low thermal conductivity. Comparison in the thermal conductivity among the common traditional insulation materials and glass foams; PUR shows the lowest values down to 20 mW m^{-1} K^{-1} while the remaining materials and glass foam obtain values in the range 30–40 mW m^{-1} K^{-1} [2,4]. For the state-of-the-art materials, the thermal conductivity can be as low as 4 mW m^{-1} K^{-1} for VIPs [2,5]. The organic and inorganic insulation materials have different properties. One important advantage of the inorganic ones is the fire resistance. In contrast, if PUR burns it raises a health issue due to the release of toxic gases [2]. Regarding the living-to-house area ratio, load-bearing insulation materials such as glass foams have an advantage over both mineral wool and organic materials due to the higher compressive strength of glass foams. From a sustainable point of view, glass foams are of great interest as they can be produced from various types of glass waste.

For many years, glass waste was used in closed-loop recycling, e.g., old window glass was remelted into new windows, glass bottles were remelted into new bottles, cathode ray tube (CRT) glass was used in new CRT glasses, etc. However, as new technologies and products are replacing old solutions, open-loop recycling is necessary to avoid landfilling of the old products. An example of this is the development of light emitting diodes (LEDs) and liquid crystal displays (LCDs) that substituted the CRT glass in televisions and computer screens [6,7]. Such CRT glass consists of four parts that by weight are 65 % panel glass, 30 % funnel glass, 5 % neck

glass, and <1 % frit glass [8,9]. Those parts have different chemical compositions. The funnel, neck, and frit glass contain large amounts of lead oxide making them difficult to recycle due to the toxicity of lead [10]. Therefore, these parts have to undergo lead removing processes such as alkaline leaching [11], carbothermal treatment [12], or smelting processes [13] before being recycled. In contrast, CRT panel glass can be directly reused as it was produced lead free after 1995 [14].

Glass foam can be used as insulation material as mentioned previously, but also as lightweight aggregate in, e.g., concrete [15] and road embankments [16]. As an insulation material glass foam benefits from the non-flammability, chemical and thermal stability, and closed porosity that makes glass foams water proof [17]. Moreover, glass foams exhibit a long life time [18]. These properties and the fact that glass foams can be produced from various types of waste glass make glass foams interesting for further research.

1.1. BACKGROUND

Foams of glassy systems have mainly been studied during melting processes where foam layers cause problems due to higher energy requirement to obtain a bubble free glass melt as the foam decreases radiative heat transfer in the melting furnace [19–23]. The foaming depends on the heating rate [24]. The lifetime of the foam depends on the processing temperature due to the influence on the glass viscosity; hence, a higher processing temperature causes a shorter foam lifetime [19,25]. This is due to coalescence of bubbles or pores, and therefore, the size distribution of bubbles depends on the melting temperature [26]. It has been shown that evaporation of oxides like Na_2O might cause a stabilization of foams at the melt surface with increasing melting temperature [25] and the higher melting temperature causes higher energy costs. During glass melting the main foaming occurs from decomposition of carbonates, hydroxyls, sulfates, etc. or oxidation reactions [19–21] which is basically the same processes used for producing glass foams.

Research in glass foams can be divided into two categories: industrial and academic. Glass foams have been known since the 1930s [27–29], but based on the amount of publications the interest did not begin before 2000 [30]. This is due to the commercial interest and the fact that the findings were patented by companies rather than published in scientific journal. Scientific publications started to show in the 1970s [31–33] and 1980s [34,35]. In the late 1990s and early 2000s an interest in recycling cullet into glass foams started [36–38]. In this approach, the foaming of cullet turns the waste into a new useful product.

The foaming of materials is complicated as it is affected by many controllable parameters such as temperature, time, gas pressure, and gas atmosphere. The process parameters need to be optimized when changing the material type (chemical composition) and particle size especially as the composition affects viscosity and

surface tension. Furthermore, the setup needs to change depending on the material. Metallic foams are prepared from high gas pressure treatments [39,40] whereas glass foams can be prepared from chemical reactions at high temperature [28,38], dissolving gases in a molten glass during cooling [27], sol-gel processes [41–43], or freeze-drying sol-gel derived glasses [44].

The overall goal of the present PhD study is to gain knowledge on the foaming principle and understanding of the impact of the solid phase (amorphous and crystalline), gas phase (composition), and pore structure (pore size and wall thickness) on the thermal conductivity of glass foams; thereby, to deepen the understanding of the insulation property. The project is part of a larger interdisciplinary collaboration between Aalborg University, Jožef Stefan Institute, and Gråsten Brickworks. The overall goal of the project is to build a house of sandwich structured building blocks consisting of clay bricks and glass foam, a so-called CleanTechBlock.

1.2. THESIS OBJECTIVE

The objectives of the present PhD study are summarized in the following four points:

1. Chemical foaming: Studying additives to a common glass-foaming agent mixture to obtain closed porous glass foams.
2. Physical foaming: Investigating the foaming mechanism with regard to build-up pressure and size of the gas specie.
3. Revealing the influence of solid matrix and gas composition on thermal conductivity of glass foams.
4. Exploring the influence of pore size on glass foam characteristics such as porosity and thermal conductivity.

1.3. THESIS CONTENT

This is an article-based thesis meaning that the thesis itself is an extended summary combined with the below mentioned papers published or submitted to international peer-reviewing journals. This thesis consists of the present six chapters and five first-authoring journal papers. Throughout the thesis, the first-authoring papers are cited using the roman numbers given below.

I. **M.B. Østergaard**, R.R. Petersen, J. König, H. Johra, and Y. Yue, "Influence of foaming agents on solid thermal conductivity of foam glasses prepared from CRT panel glass", *Journal of Non-Crystalline Solids*, **465** (2017), 59-64.

II. **M.B. Østergaard**, R.R. Petersen, J. König, and Y. Yue, "Effect of alkali phosphate content on foaming of CRT panel glass using Mn_3O_4 and carbon as foaming agents", *Journal of Non-Crystalline Solids*, **482** (2018), 217-222.

III. **M.B. Østergaard**, R.R. Petersen, J. König, M. Bockowski, and Y. Yue, "Foam glass obtained through high-pressure sintering", *Journal of the American Ceramic Society*, **101** (2018), 3917-3923.

IV. **M.B. Østergaard**, B. Cai, R.R. Petersen, J. König, P.D. Lee, and Y. Yue, "Impact of pore structure on thermal conductivity of glass foams", *Materials Letters, under review*

V. **M.B. Østergaard**, R.R. Petersen, J. König, M. Bockowski, and Y. Yue, "Impact of gas phase on thermal conductivity of glass foams", *Journal of Non-Crystalline Solids, under review*

CHAPTER 2. CHEMICAL FOAMING

Glass foams can be produced by different processes. The most common production is based on a chemical approach where glass powder and foaming agents are mixed and heated. This is the method used to prepare glass foams in Paper II and Paper IV, and it is described in the following chapter.

2.1. SAMPLE PREPARATION PROCEDURE

Glass is crushed to obtain small particle size. Glass powder and foaming agents are mixed using a ball mill to homogenize the mixture and decrease the particle size as the particle size has a great impact on foaming ability and foam characteristics [45]. The powder mixture is uniaxially pressed into a pellet at 40 MPa as shown in Figure 2.1 as samples prepared from compacted powder mixtures obtain a more uniform structure than samples prepared from loose powder mixtures [28]. The pellets can have diameters of 13 mm or 35 mm.

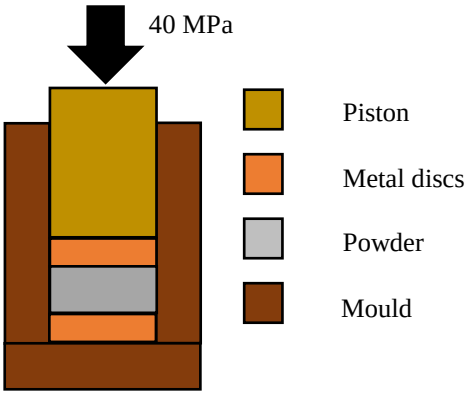

Figure 2.1 Method for uniaxial pressing of powder mixtures. The diameter of the mould can be either 13 mm or 35 mm.

The foaming of the pellets was carried out in two different ways. Small pellets (1 g, Ø = 13 mm) were placed on a kaolin coated alumina plate and foamed in a heating microscope. Large pellets (20 g, Ø = 35 mm) were placed on a stainless steel plate in a circular mould of 60 mm diameter covered with alumina-silica fibers to prevent sticking and foamed in an electrical heated tube furnace with gas control.

2.2. PRINCIPLE OF CHEMICAL FOAMING

Foaming of glass powder using foaming agents involves different steps. After the mixing and compression into a pellet, the mixture is heated. During the heating, the mixture reaches the sintering point of the glass that is an essential step towards making

a foam. The sintering causes a closed body that can entrap gas which is released from the foaming agents rather than releasing the gas to the surroundings. Continuing the heating, the glass phase reaches the softening point (viscosity of $10^{6.6}$ Pa s); hereafter reactions of the foaming agents should occur. The reactions can be either decomposition of metal carbonates, reaction between glass and foaming agents, or reactions between multiple foaming agents. These reactions result in gas release which will expand the viscous body. Further heating will cause coalescence of the pores and eventually a foam collapse, while cooling will freeze the obtained pore structure resulting in a glass foam [28]. The right temperature program is important and depends on both the glass and the foaming agents. In general MnO_2 and metal carbonates are found to have the optimum foaming in the viscosity window 10^4–10^6, while SiC requires a lower viscosity of $10^{3.3}$–10^4 for different glass compositions [46].

2.2.1. METAL CARBONATES

Foaming of glass has been carried out using several different foaming agents. Some of the most popular based on literature are metal carbonates, mainly $CaCO_3$ [46–54], though, Na_2CO_3 [53–57], $MgCO_3$ [58], and $SrCO_3$ [34,58] are also described in literature. $CaCO_3$ and $MgCO_3$ is often added as minerals, calcite ($CaCO_3$) [59,60] or dolomite ($CaMg(CO_3)_2$) [59–61], or waste products as egg shells ($CaCO_3$) [50,59,62,63] or oyster shells ($CaCO_3$) [64]. Metal carbonates decompose upon heating producing CO_2 and their metal oxide counterpart, e.g., Na_2O and CaO as shown in Equation 2.1, where M = Na, Ca, Mg, Sr etc.

$$M_xCO_3(s) \rightarrow M_xO(s) + CO_2(g) \tag{2.1}$$

Foaming experiments of CRT panel glass and Na_2CO_3 showed that the expansion of the glass melt occurs prior to the decomposition temperature of pure Na_2CO_3 caused by reaction between the glass and Na_2CO_3 [57]. This is also found for $CaCO_3$ [48] and is, therefore, probably the case for other carbonates as well. After the decomposition of the metal carbonate, the metal oxide is incorporated into the glass structure lowering the glass transition temperature (T_g) due to a fluxing effect or causing crystallization. Crystallization can occur as the foaming agent provides nucleation sites. This is observed for a CRT panel glass and Na_2CO_3 system [56,57].

2.2.2. TRANSITION METAL OXIDES AND CARBONACEOUS COMPOUNDS

Glasses can be foamed using transition metal oxides, carbonaceous compounds, or combinations. Foaming using these compounds depends on oxidation of carbonaceous compounds or reduction of transition metals in order to produce gas. SiC is a commonly used foaming agent either alone where it is oxidized by the air or redox-reactions in the glass [34,65–68], but also in combination with Fe_2O_3 or Co_3O_4 [34,65,69], MnO_2 [68], and CuO or NiO [34]. Other foaming agents are MnO_2 alone

[70–73] or combined with Si_3N_4 [74] and Mn_xO_y with carbon [45,75–77]. The disadvantage of using SiC compared to metal carbonates or manganese oxides is the requirement of higher temperature as SiC needs a lower viscosity in order to cause expansion [46]. The Mn_3O_4 and carbon combination has shown superior properties. The reactions between the foaming agents and the CRT panel glass can be divided into three stages: 1) a solid-solid reaction between Mn_3O_4 and carbon, 2) a melt-reduction, i.e., reduction of polyvalent ions in the glass melt, and 3) a dissolution-reaction, where Mn_3O_4 dissolves into the glass melt and the dissolved Mn^{3+} ions reduce releasing oxygen [77]. The solid-solid reaction follows Equation 2.2.

$$4Mn_3O_4(s) + 2C\ (s) \rightarrow 12MnO(s) + 2CO_2(g) \tag{2.2}$$

As for the metal carbonates, the remaining transition metal oxides will either dissolve into the glass melt [73] or exist as crystals in the solid matrix [72,73]. Similarly, a combination of Fe_2O_3 and carbon reacts as in Equation 2.2. In the case of Fe_2O_3, the remaining Fe_2O_3 and FeO is either dissolved in the glass phase or causing crystallization of the glass [78]. Therefore, depending on the foaming agent, small differences are found in their reactions with the glass. Moreover, the type of glass has a significant influence on crystallization probability as different glass compositions have different tendency to crystallize. The combination of Fe_2O_3 and carbon in CRT panel glass shows no crystallization whereas the same combination in flat glass results in crystallization [78].

2.3. EFFECT OF ALKALI PHOSPHATES ON FOAMING OF CULLET

The structure and properties of foams can be altered by addition of different additives. Among reported additives, TiO_2 has been used as nucleation agent [76] and oxidant [79] in glass foams, while phosphates have shown a foam stabilizing effect when foaming metallurgical slags [80]. Sodium phosphates in various types have been adopted in glass foams and claimed to be a foam stabilizer in several studies. Among such phosphates are $Na_3PO_4{\cdot}12H_2O$ [81–83], Na_3PO_4 [84], and Na_2HPO_4 [47,85]. However, the effect of phosphates on glass foams was never investigated. In Paper II, we investigated the effect of a series of alkali phosphates on the foaming and foam structure of glass foams prepared from CRT panel glass, Mn_3O_4, and carbon. The used alkali phosphates were Li_3PO_4, Na_3PO_4, and K_3PO_4.

All the tested alkali (Li, Na, and K) phosphates show similar effect on the foaming behavior, however, the effect is more explicit for smaller ions (Figure 2.2). The foaming temperature (T_{foam}), described as the minimum in silhouette area (A/A_0), decreases with increasing content of alkali phosphate with the largest change occurring for Li_3PO_4 containing samples. This is caused by the fluxing effect of the alkali ions among these, the Li^+ ions diffuse faster compared to Na^+ and K^+ ions [86,87]. With increasing temperature, the silhouette area increases due to the foaming of the samples. When reaching the maximum temperature (804 °C), the samples are

exposed to an isothermal heating for 15 min. During the isothermal heating, the samples behave differently. For the Li_3PO_4 containing samples (≥0.34 mol%), the foam collapses due to pore coalescence and bursting of surface pores. The same phenomenon occurs in samples with high content of Na_3PO_4 (≥0.86 mol%), whereas the K_3PO_4 containing samples continuously expand. This difference can be explained by the difference in viscosity for the samples as small ions cause a larger decrease in viscosity [88]. At low viscosity it is easier for the gas to escape the glass melt. During the cooling, all samples shrink due to a decrease in pressure inside the pores and the normal volume change of melts with decreasing temperature.

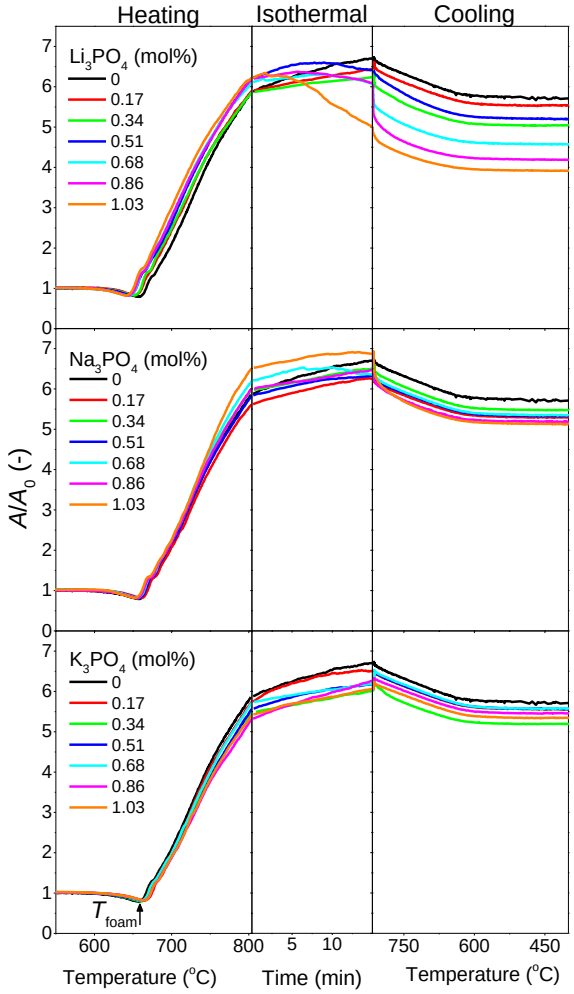

Figure 2.2 Change in sample size measured as change in silhouette area (A/A_0) during heating (left), isothermal treatment (center), and cooling (right). Figure is from Paper II.

The difference in final size of the glass foams shown in Figure 2.2 is directly reflected in the porosity (Figure 2.3a). A significant decrease in porosity is found for the Li_3PO_4 containing samples at concentrations ≥0.34 mol% compared to Na_3PO_4 and K_3PO_4 due to the foam collapse. A similar decrease is observed for Na_3PO_4 containing samples at concentrations ≥0.86 mol%, though, this is not as dramatic. In contrast, the K_3PO_4 containing samples do not vary in porosity with increasing K_3PO_4 concentration. In relation to the porosity, the closed porosity is important in order to entrap low thermal conducting gases in glass foams. The K_3PO_4 containing samples exhibit closed porosity similar to the sample without any alkali phosphate added (Figure 2.3b) indicating that K_3PO_4 could be added to maintain a high closed porosity without compromising the porosity. In contrast, the closed porosity decreases for samples containing Na_3PO_4 (≥0.86 mol%) and Li_3PO_4 (≥0.34 mol%). Therefore, the temperature program needs to be optimized, i.e., lower temperature or vary the isothermal heat-treatment, to avoid the foam collapse.

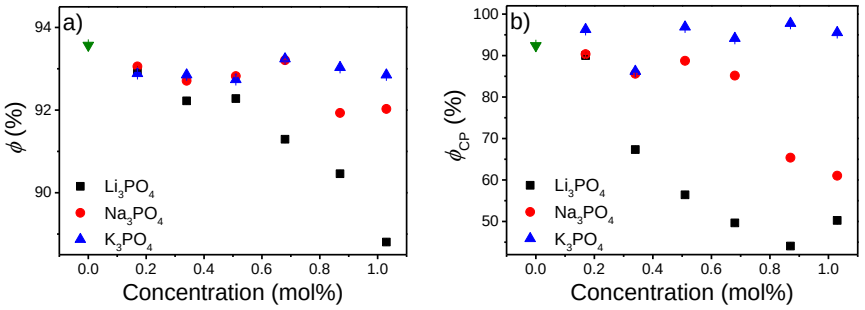

Figure 2.3 a) Porosity (ϕ) and b) closed porosity (ϕ_{CP}) of glass foams prepared from CRT panel glass, Mn_3O_4, carbon with either Li_3PO_4, Na_3PO_4, or K_3PO_4. Figures are from Paper II.

The fluxing effect of the alkali ions from the alkali phosphates is suggested as the reason for the foam collapse. Changes in T_g of the crushed glass foams (Figure 2.4) support this fluxing effect. The T_g is lowered by up to 32 °C for the highest content of Li_3PO_4 which is a significantly larger drop in T_g compared to Na_3PO_4 and K_3PO_4 containing samples. This is in agreement with the literature [89,90]. It is interesting that the T_g is similar for glass foams containing Na_3PO_4 and K_3PO_4. Only the high content Na_3PO_4 samples (≥0.86 mol%) collapse during the isothermal heat-treatment while all K_3PO_4 containing samples withstand the heat-treatment. This similar effect of Na_3PO_4 and K_3PO_4 on the T_g might be caused by the relatively high content (>7 wt%) of each alkali oxide in the CRT panel glass [73] in addition to the other modifying oxides. In contrast, Li_2O is not found in the CRT panel glass and that in combination with the higher diffusivity of Li^+ ions causes the lower T_g. Moreover, the small difference between the Na_3PO_4 and K_3PO_4 containing samples indicates that other phenomena such as surface tension might affect the foam collapse of the Na_3PO_4 containing samples. K_3PO_4 and Li_3PO_4 are found to have a significant effect at 1400

°C whereas Na_3PO_4 has no influence on the surface tension [91]. The foaming occurs at lower temperature (maximum temperature 804 °C), however, even at this lower temperature there might be a difference in the behavior of K_3PO_4 and Na_3PO_4 on the surface tension.

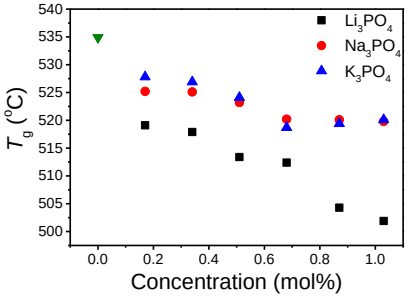

Figure 2.4 Glass transition temperature (T_g) of crushed glass foams prepared from CRT panel glass, Mn_3O_4, carbon with either Li_3PO_4, Na_3PO_4, or K_3PO_4. Figure is from Paper II.

The proposed foam stabilizing effect especially of sodium phosphates should be seen in the pore structure. However, as seen in Figure 2.5, the pore structure does not obtain a more homogeneous pore size, pore shape, or wall thickness when adding alkali phosphates up to 1.03 mol% to the CRT panel glass, Mn_3O_4, and carbon mixture. Therefore, the alkali phosphates should not be added in order to improve the macroscopic structure of glass foams.

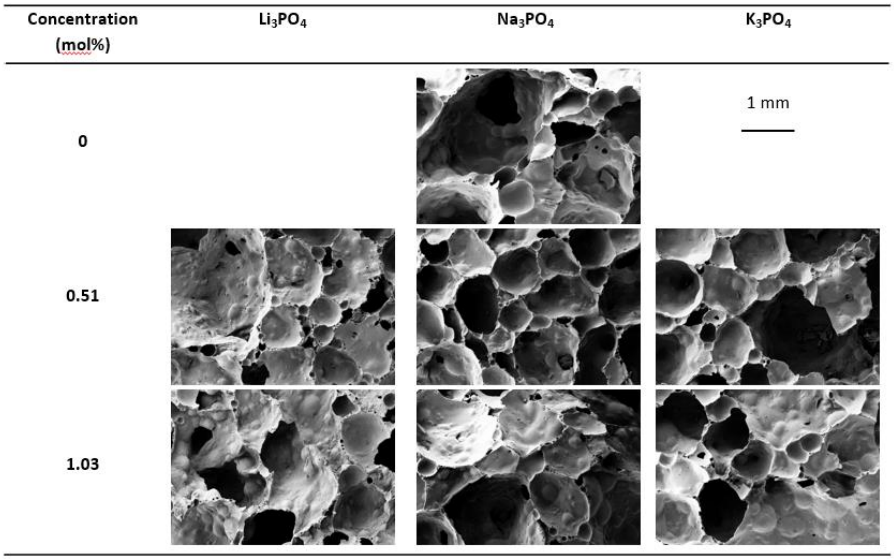

Figure 2.5 SEM images of the pore structure of selected glass foams prepared from CRT panel glass, Mn_3O_4, carbon, and either Li_3PO_4, Na_3PO_4, or K_3PO_4. Figure is from Paper II.

2.4. KEY PARAMETERS FOR CHEMICAL FOAMING

The chemical foaming depends on various parameters. First of all, the decomposition or reaction temperature of the foaming agents has to be in the right viscosity range of the glass used [28,46]. The glass needs to sinter before the gas release of the foaming agents, while the foaming agents need to decompose before the viscosity of the glass becomes too low to entrap the gas. Therefore, the temperature is crucial to control and it needs to be varied for different glass compositions. As seen in Figure 2.2, the Li^+ and Na^+ ions from the alkali phosphates cause foam collapse due to a fluxing effect. If the processing temperature for these samples was decreased, closed porous glass foams could have been obtained as the foam collapse would not have occurred. In relation to the temperature, the heating rate is important. A low heating rate is preferable in order to heat the sample uniformly [28]. A heating rate of 5–10 °C min^{-1} is previously suggested [28], though, comparing a heating rate of 5 °C min^{-1} and 10 °C min^{-1}, a lower foam density is obtained when decreasing the heating rate [45].

In order to prepare thermal insulating glass foams, low density (or high porosity) is crucial. In order to obtain this, the particle size of the powder and foaming agents can be reduced as this improves the foaming [28,45]. As the size of the foaming agent decreases, the total surface area increases which increases the reaction kinetics. The initial particle size also affects the pore size in the glass foams [28].

2.5. SUMMARY

Chemical foaming can be performed using different foaming agents usually divided into metal carbonates and transition metal oxides and/or carbonaceous compounds. The main principle of all is the same, where glass powder containing foaming agents is pressed into a green body and heated above the softening point. The glass powder sinters forming a closed body which entrap the gases produced from the foaming agents either through decomposition or redox-reaction.

Additives can help alter the foaming procedure or foam characteristics. Alkali phosphates as additives show a significant effect on the foaming when changing both the alkali part among Li, Na, and K and the concentration (up to 1.03 mol%). Neither of the alkali phosphates show an effect on the pore structure, i.e., pore size, pore shape, and wall thickness, within the investigated range of concentration. However, K_3PO_4 shows promising results in order to obtain a high degree of closed pores for highly porous glass foams.

CHAPTER 3. PHYSICAL FOAMING

Other approaches than the chemical foaming are used to produce glass foams. The metal foam industry uses a process based on high pressure sintering [40,92,93]. In order to understand the foaming of glass foams, a similar approach has been tested [94]. The physical foaming is described in this chapter and used to produce glass foams in Paper III and Paper V.

3.1. PRINCIPLE OF PHYSICAL FOAMING

The physical foaming approach used by Wang et al. [94] is a two-step procedure in contrast to the one-step chemical foaming. Glass powder is pressed into a pellet as described in Section 2.1, though, without any foaming agent. The pellet is sintered under gas pressure. The sintering forms a closed body where a high gas pressure is entrapped. Subsequent reheating results in expansion due to the high internal gas pressure and the decrease in viscosity of the glass. The heat-pressure program of the samples in Paper III and Paper V is shown in Figure 3.1. For samples in Paper V, the reheating is performed multiple times to an increasing maximum temperature in order to obtain similar chemistry in the gas and solid phases, though, with different density.

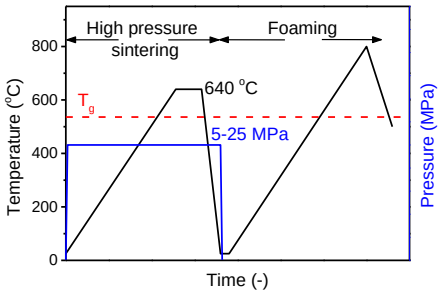

Figure 3.1 Illustration of the high-pressure sintering and rehating program of glass foams prepared by a physical foaming approach. Figure is from Paper III.

3.2. EFFECT OF GAS AND PRESSURE ON PHYSICAL FOAMING

Physical foaming is greatly affected by both the gas specie and the pressure used during sintering. Considering the gas specie, only Ar is found in literature [94] while different gases (He, Ar, and N_2) is investigated in Paper III and Paper V. The foaming process is for the first time described in Paper III as both Wang et al. [94] and Paper V focus on the structure or properties of the glass foams. Foaming characteristics of samples from Paper III are shown in Figure 3.2. First, considering the gas specie, the Ar- and N_2-sintered samples expand up to 600 % before cooling while the He-sintered

samples expand up to 200 % (Figure 3.2b). Among these three gases, He has the highest solubility in glasses [95] probably due to the smaller kinetic diameter. The kinetic diameter of He, Ar, and N_2 are 0.255 nm, 0.354 nm, and 0.364 nm, respectively [96]. These values show that He fits into the silicate rings if these are not occupied by modifying ions. Moreover, a large amount of He can be physically dissolved into the glass structure [97–100], rather than being entrapped in the closed pores of the sintered pellet. Hence, a lower pressure exists in the pores limiting the expansion of the glass melt. Another possibility of the small expansion of the He samples is that He is released from the sample during heating as it can escape the glass structure through the interstitial solubility sites. In contrast, Ar and N_2 are too large to fit into the interstitial sites and are, therefore, entrapped in the closed pores, increasing the pressure, and thus, resulting in a larger expansion. The foaming of the samples starts between 540–585 °C for all samples (Figure 3.2a), when the onset foaming ($T_{foaming}$) is defined as $A/A_0 = 1.05$. In general, the He-sintered samples start foaming at a lower temperature followed by the Ar-sintered and N_2-sintered ones. Hence, the $T_{foaming}$ follows the kinetic diameter of the gases. A reason for this could be the easier diffusion of He compared to the other gases which makes it easier to move at high viscosities.

Secondly, the gas pressure shows a significant effect on the $T_{foaming}$ and maximum expansion (Figure 3.2). In general, the foaming initiates at lower temperatures with increasing pressure as the higher internal forces can expand a more viscous melt than lower forces at low pressure. In contrast, the pressure effect shows a maximum foaming at 20 MPa, while samples sintered at 25 MPa foam less. This might be due to the forces created by the internal pressure overcoming the force of the glass melt, e.g., surface tension and viscosity, and the external atmospheric pressure.

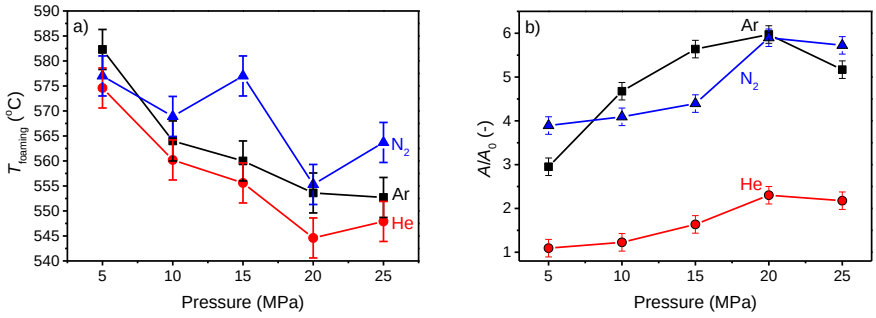

Figure 3.2 a) Foaming temperature ($T_{foaming}$) defined by $A/A_0 = 1.05$ and b) maximum expansion during heating. Figures are from Paper III.

Comparison of maximum foam size at maximum temperature is difficult as the foams shrink during cooling. However, the final glass foams can be compared among various studies as the final size is related to the porosity. The porosity of samples prepared by physical foaming in Paper III, Paper V, and by Wang et al. [94] all suggest a critical pressure during sintering around 20 MPa (Figure 3.3). The shown porosities

are for single heat-treated samples. Hence, the samples from Paper V are heat-treated at much lower temperature than the samples from Paper III. The difference in foaming temperature explains the difference in porosity between the two Ar-sintered series and between the two N_2-sintered series.

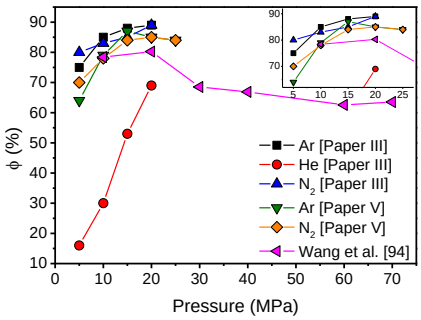

Figure 3.3 Porosity (ϕ) of glass foams prepared from CRT panel glass sintered in He, Ar, and N_2 at gas pressures of 5-20 MPa from Paper III, Ar and N_2 at gas pressures of 5-25 MPa from Paper V, and borosilicate glass sintered in Ar at gas pressures of 10-70 MPa obtained by Wang et al. [94]. *The difference between Ar- and N_2-sintered samples form Paper III and Paper V is the heating process. Inset is a zoom-in on the 5-25 MPa area with high porosity samples.*

The physical approach makes it possible to entrap gases inside the glass foams that are not possible to entrap chemically. Gas analyses of the Ar- and N_2-sintered samples show large amounts of the sintering gas (>70 vol%). However, CO_2 is present with up to 30 vol% (Table 3.1), plausibly caused by oxidation of carbon particles from the experimental setup. The high CO_2 content in the Ar- and N_2-sintered samples suggest that the He-sintered samples also contain CO_2. The He-sintered samples are possibly foamed by the development of CO_2 rather than being caused by a He pressure. Also, the CO_2 development has enhanced the expansion of the Ar- and N_2-sintered samples.

Table 3.1 Normalized gas composition ($V_{Ar} + V_{CO2} = 1$ and $V_{N2} + V_{CO2} = 1$) (vol%) of glass foams heat-treated seven times with 15 °C increamentals from 650 °C to 740 °C. The table is modified from Paper V.

Gas type	Pressure (MPa)	Ar (vol%)	CO_2 (vol%)	N_2 (vol%)
Ar	5	69.9	30.1	-
	10	70.5	29.5	-
	15	76.5	23.5	-
	20	71.6	28.4	-
N_2	5	-	16.1	83.9
	10	-	17.0	83.0
	15	-	12.2	87.8
	20	-	13.4	86.6

3.3. KEY PARAMETERS FOR PHYSICAL FOAMING

The research conducted on physical foaming of glass foams is limited, hence, a lot of work has to be done to get as thorough an understanding as for the chemical foaming. However, for now some initial parameters are understood. It is found that larger gas species, whether it is noble or molecular gases, seem to increase the size of the glass foams. Therefore, larger gas species than N_2 could be investigated in order to find a possible maximum size of gas specie or relate the kinetic diameter (or other size relevant parameter) to the size of the final glass foam. In contrast, the sintering pressure is found to have an optimum at 20 MPa based on results obtained by Wang et al. [94], Paper III, and Paper V. Therefore, sintering at 20 MPa using large inert gas species is for now the known key parameters.

3.4. SUMMARY

Glass foams prepared through a physical foaming approach demonstrate the importance of the pressure that is build up inside the glass pellet. If the pressure is low, the expansion will be limited, while too high internal pressure will cause bubble bursting and eventual foam collapse. Also, the pressure shows great importance for the rate of expansion. Even though glass foams produced from a physical approach are pre-sintered under high gas pressure prior to foaming, the theory can be used in the chemical foaming as glass foams prepared from chemical foaming undergo a sintering process prior to reaction of foaming agents or at least prior to entrapping gases of the reacting foaming agents. The kinetic of the reaction in the chemical foaming is important in order to build up a pressure that causes expansion of the glass melt.

CHAPTER 4. THERMAL CONDUCTIVITY OF GLASS FOAMS

For insulating purposes, the thermal conductivity of the glass foams is a crucial property. The thermal conductivity decreases linearly with decreasing density (and thus increasing porosity) for cellular materials [71,73,101–106]. However, comparing data from different studies is almost impossible as different parameters affect the measurements, e.g., temperature, but also lack of information about the samples measured, e.g., chemical composition (both solid and gas phase), crystallinity, and closed porosity. The following sections describe the effect of solid and gas phase and pore structure on the thermal conductivity of glass foams. In addition to the mentioned parts, it is known that other contributions might affect the thermal conductivity of porous solids including the solid-gas coupling [107,108], radiative heat transfer [109–111], and convection [110,112]. However, these are not investigated in the present project, and therefore, will only be described briefly.

The thermal conductivity was obtained by two different methods depending on the samples being bulk samples or glass foams. For bulk samples, the thermal conductivity was calculated from the thermal diffusivity measured by Laser Flash (LFA 447, Netzsch), the heat capacity (C_p) measured by differential scanning calorimetry (DSC; STA 449C, Netzsch), and the bulk density. Glass foams were measured with a transient plane source technique (TPS 2500 S, Hot Disk AB) where the glass foams were placed in a climate chamber to control the temperature.

4.1. RADIATION, CONVECTION, AND GAS-SOLID COUPLING

The radiative heat transfer is a difficult measure as it depends on porosity, chemical composition of both solid and gas phase, thickness of cell walls and struts, and the shape of pores [113]. Thermal radiation consist of the infrared (IR), visible, and ultraviolet (UV) light [114]. In glass melting systems, the foam layer is found to cause scattering of the near-IR waves [19]. When a sample is exposed to IR, visible, or UV light, the thermal radiation of the sample depends on the amount of light absorbed, reflected, or transmitted. The transmittance is often neglected for solids and liquids [114]. The porous nature of glass foams makes the total porosity important for the thermal radiation as it decreases with decreasing porosity for different organic foams [109,111] and glass foams [109]. However, the contribution from radiation usually is in the range of 5 to 20 % for glass foams [109]. Glass foams often consist of a silicate glass skeleton that are almost complete opaque to near- and mid-IR light. Also, the high conductive of the solid phase makes the foam density the most important parameter [115]. In contrast, the thermal radiation of the gas phase depends

on the size of the gas molecules. Monatomic and diatomic gases are transparent to radiation whereas polyatomic gases absorb radiation [114].

The convection in cellular materials are found to be neglectable for pores less than 4 mm in diameter [110,112]. For convection and pore size, the Knudsen's effect plays a role when either the pore size or gas pressure is reduced [116,117]. The Knudsen's effect is pronounced for aerogels as the Knudsen's number (ratio of the mean free path for gas molecules to average pore size) increases with decreasing average pore size resulting in a decrease in thermal conductivity [118]. Moreover, the Knudsen's effect only depends on the size of the pores and not their morphology [119]. In general, the thermal conductivity decreases with decreasing pressure for gases [120,121]. The effect of gas phase and pore size are further discussed in Sections 4.3 and Section 4.4, respectively.

The solid-gas coupling of porous materials is not well understood and is rarely mentioned for glass foams. It exist on the boundary between the glass skeleton and the pore and depends on the ratio of the distance the heat is transferred within the solid and gas phase [107]. The solid-gas coupling has been investigated for aerogel systems [107,108,122,123]. The contribution to the thermal conductivity by the solid-gas coupling is enlarged when the relative solid contribution increases [107], hence, for high porosity glass foams it should be low. Furthermore, the coupling contribution increases with the ratio of thickness of solid phase to mean pore size [107]. Glass foams tend to have thin walls compared to the size of the pores based on 2D and 3D images of glass foam structures in literature [51,73,124]. Wall thickness-to-pore size ratios are previously reported in the range of 0.05–0.09 for glass foams [102], meaning the pores are significantly larger than the walls. Finally, a higher gas pressure increases the thermal contribution from the solid-gas coupling [107]. The cell pressure in glass foams is only reported in a single study to the knowledge of the author showing values around 0.40 bar [78].

4.2. SOLID PHASE CONTRIBUTION

It is well-known that the thermal conductivity of pure crystals is higher than their amorphous counterparts [125–127]. However, the contribution of solid phase to the thermal conductivity of glass foams is limited [76]. The majority of the solid phase is amorphous. Therefore, the influence of chemical composition is of interest, but the literature is limited [128]. Data from, e.g., Ghoneim et al. [126], Salman et al. [129,130], and van Velden [131] were combined by Choudhary and Potter who made a linear statistical model [132]. This empirical model describes the thermal conductivity based on chemical composition, but within small regions due to the limited data. Using the chemical composition of post-consumer glasses (float, bottle, and CRT panel) the thermal conductivity of the CRT panel glass is around 12 % lower than that of the float and bottle glass [30]. Furthermore, glass foams prepared from CRT panel glass rather than float glass show lower thermal conductivity when using

the same foaming agents [78]. Therefore, CRT panel glass is interesting for glass foams used as thermal insulation. However, the solid phase of glass foams often contain crystals as the glass crystallize during heat-treatment [68,133] or foaming agents either cause partly crystallization of the glass [52,56,57,60,134] or remain in the glass matrix [72,73]. However, the thermal conductivity of glass-ceramics and amorphous matrices with crystals embedded is limited. The incorporation of small particles, e.g., crystallites into a glass matrix can cause scattering of the phonons during the heat transport through the sample. The phonon scattering acts as a thermal barrier that causes a decrease in the overall thermal conductivity of the sample [135–138]. Hence, the presence of crystallites in an amorphous matrix might improve the thermal insulation of glass foams.

The effect of crystal content on the thermal conductivity of the solid phase was investigated in Paper I. Samples were prepared by melt-quenching and sintering to obtain samples with the foaming agent fully incorporated into the glass structure and samples with the foaming agent partly dissolved into the glass structure, respectively. XRD patterns show a high crystalline content in the powder mixtures. The diffraction peaks are significantly lower for the sintered samples while the melt-quenched samples appear fully amorphous as seen for some MnO_2 containing samples in Figure 4.1. The CRT panel glass does not crystallize, hence, both the melt-quenched and the sintered ones are amorphous.

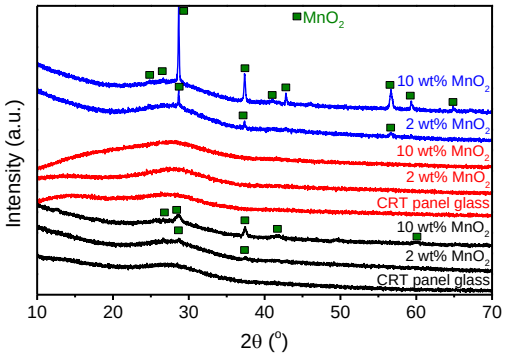

Figure 4.1 XRD patterns of either the powder mixture (blue), melt-quenched samples (red), or sintered samples (black) of CRT panel glass and MnO_2 mixtures. Data are from Paper I.

The density of the melt-quenched samples increases linearly from 2.75 g cm^{-3} (pure CRT panel glass) to 2.8 g cm^{-3} and 2.85 g cm^{-3} for samples with Fe_2O_3 (0–6 wt%) and MnO_2 (0–10 wt%), respectively (see Paper I). The sintered samples are more complex than the melt-quenched ones as they are porous. The density increases with increasing content of either Fe_2O_3 or MnO_2. However, for thermal conductivity measurements, the porosity is important. The porosity is <10 % for all sintered samples with no link to composition (Figure 4.2).

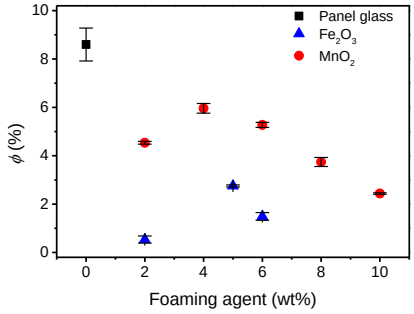

Figure 4.2 Porosity (ϕ) of the sintered samples with increasing content of foaming agent (MnO_2 or Fe_2O_3). Figure is from Paper I.

The thermal conductivity of sintered (partly crystalline) samples can be corrected for their porosity using Equation 4.1, which is useful for low porosity materials [139]. λ_{solid} is the thermal conductivity of the solid phase and λ_{meas} is the value obtained from experiments. The melt-quenched samples are non-porous, hence, $\lambda_{meas} = \lambda_{solid}$.

$$\lambda_{meas} = \lambda_{solid}(1 - \frac{4\phi}{3}) \quad (4.1)$$

The thermal conductivity increases with increasing content of foaming agent in the sample for both MnO_2 and Fe_2O_3 (Figure 4.3). The range of thermal conductivity is slightly different as the melt-quenched samples obtain values in the range of 0.8–1.3 W m^{-1} K^{-1}, while the sintered ones have a larger range of 0.8–1.5 W m^{-1} K^{-1}. In general, the values are within the typical range of silicate glasses [140]. Comparing this trend to literature, the increase in thermal conductivity with increasing Fe_2O_3 content is in agreement with the model proposed by Choudhary-Potter [132]. In contrast, the literature disagrees on the effect of MnO_2. Ghoneim et al. [126] shows an increase in thermal conductivity with increasing MnO content, whereas Choudhary-Potter [132] shows a decrease in thermal conductivity with increasing MnO content. However, the literature results are based on small amounts of MnO (<0.10 wt%) which is much lower content than used in the samples presented here.

The thermal conductivity of the melt-quenched and the sintered CRT panel glass samples is similar (Figure 4.3). In contrast, the thermal conductivity of the sintered samples containing foaming agents is higher than their respective melt-quenched ones. Hence, the difference in the thermal conductivity between sintered and melt-quenched samples must be due to the crystal content and different incorporation into the glass structure. It is also clear that the crystal size is too large to cause phonon scattering as that would have resulted in a lower thermal conductivity of the sintered samples compared to the melt-quenched ones. It can be concluded that the crystal size needs to be tailored or crystals should be avoided in order to improve the insulating performance glass foams.

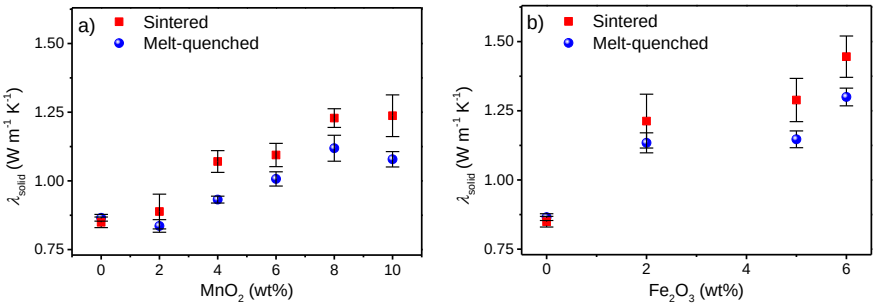

Figure 4.3 Solid thermal conductivity (λ_{solid}) of CRT panel glass melt-quenced or sintered with a) MnO_2 or b) Fe_2O_3. Figures are from Paper I.

4.3. GAS PHASE CONTRIBUTION

Glass foams with controlled chemistry were prepared by physical foaming as described in Chapter 3. The glass foams were prepared by sintering of glass powder at 5–20 MPa gas pressure using Ar or N_2. The gas compositions of the glass foams are found in Table 3.1 showing the sintering gas (Ar or N_2) and CO_2 in the pores. As the gas phase is a binary mixture, a combined thermal conductivity of the gas phase ($\lambda_{gas,mix}$) was calculated using a model proposed by Wassiljewa [141] (Table 4.1). The compositional difference among the Ar-sintered samples is too small to give a difference in the $\lambda_{gas,mix}$ which is in agreement with literature [142]. This is also the case for N_2–sintered ones. The difference in thermal conductivity between the Ar- and N_2-series is 6.7 mW m^{-1} K^{-1}, and therefore, it can be used to find an influence on the thermal conductivity of glass foams. The gas pressure affects the thermal conductivity [121,142], however, the small difference in cell pressure (P_{cell}) shown in Table 4.1 is not expected to affect the thermal conductivity of glass foams. This is further implied by the change in thermal conductivity with changing density (Figure 4.4).

Table 4.1 Theoretical thermal conductivity of the gas mixture ($\lambda_{gas,mix}$) calculated from compositions in Table 3.1 and cell pressure (P_{cell}) calculated using Boyle's law. Table is modified from Paper V.

Gas type	Pressure (MPa)	$\lambda_{gas,mix}$ (mW m^{-1} K^{-1})	P_{cell} (bar)
Ar	5	16.4	0.20
	10	16.4	0.18
	15	16.4	0.20
	20	16.4	0.19
N_2	5	23.1	0.19
	10	23.1	0.18
	15	23.1	0.19
	20	23.1	0.17

The thermal conductivity decreases with decreasing density (Figure 4.4) in agreement with various studies [71,73,78,102,143]. The sintering pressure does not have any influence on the thermal conductivity as it is reflected in the density. Hence, an increasing pressure causes a lower density, and thus, a lower thermal conductivity. Comparing samples with similar density, there is no clear trend whether the samples sintered at higher pressure also show higher thermal conductivity, and therefore, a higher cell pressure should affect the thermal conductivity of the glass foam. The cell pressures shown in Table 4.1 are measured after the final heating. Probably the cell pressure decreases slightly for every heat-treatment as the pressure is used to expand the glass foam, hence, decrease the density.

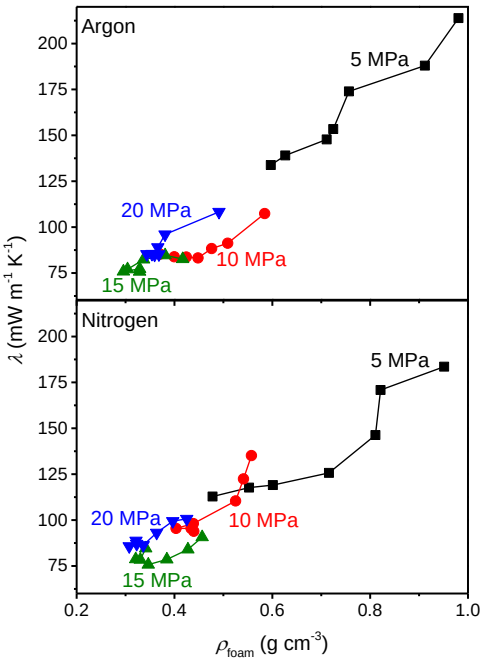

Figure 4.4 Thermal conductivity (λ) as function of density (ρ_{foam}) of glass foams prepared by a physical approach using Ar or N_2 as compression gas at 5–20 MPa during sintering. Figure is from Paper V.

As the cell pressure is suggested not to affect the thermal conductivity of the glass foams, the main difference is, except for density, the gas phase. The data from Figure 4.4 are combined in Figure 4.5 to only look at density and gas phase. Interestingly, glass foams with the N_2-rich gas phase show a lower thermal conductivity at high density (>0.6 g cm^{-3}). This can be due to the relatively low gas volume in these glass foams causing other effects as pore size and solid phase to have a higher impact. The pore size often increases to cause a decrease in density [144], and an increasing pore size is suggested to cause a lower thermal conductivity [145]. However, at low density

(<0.6 g cm^{-3}) the glass foams with Ar-rich gas phases show lower thermal conductivity compared to the ones with N_2-rich gas phases. This is in agreement with the lower $\lambda_{gas,mix}$ calculated for the gas phases. The data are scattered in the low density regime showing no clear linear decrease of thermal conductivity with decreasing density and some N_2-rich glass foams show a low thermal conductivity which all indicate other factors to play a role. In general, a low thermal conducting gas phase results in a lower thermal conductivity of glass foams. This trend will be even more pronounced for glass foams with lower density. Here, the relative gas contribution ($\lambda_{gas,mix}/\lambda$) for the samples with the lowest density is 22 % and 31 % for the Ar-rich and N_2-rich gas phases, respectively. In contrast, a chemically foamed glass foam prepared from flat glass, Mn_3O_4, carbon, and TiO_2 with density of 0.117 g cm^{-3} shows the solid and gas phase to contribute almost equally [76] showing the importance of minimizing the gaseous contribution to the thermal conductivity at low density. An increasing gas contribution is beneficial as, in general, the thermal conductivity of gases are lower than solids. CRT panel glass has a thermal conductivity of 925 mW m^{-1} K^{-1} [73] whereas Ar, CO_2, and N_2 has thermal conductivities of 17.6 mW m^{-1} K^{-1} [146], 16.3 mW m^{-1} K^{-1} [147], and 26.4 mW m^{-1} K^{-1} [148], respectively.

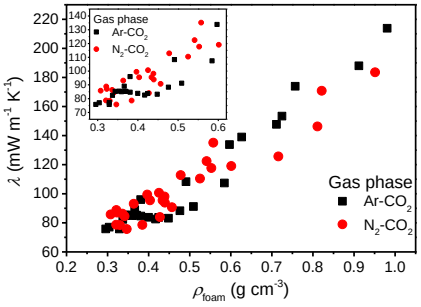

Figure 4.5 Thermal conductivity (λ) of glass foams with differenct binary gas phases (Ar-CO_2 or N_2-CO_2). Inset shows the low-density area (<0.6 g cm^{-3}). Figure is modified from Paper V.

4.4. MACROSTRUCTURAL EFFECT

The effect of pore structure of glass and glass-ceramic foams on thermal conductivity is only briefly studied in literature. Köse and Bayer [35] showed both theoretically and experimentally that for low density glass foams (<0.4 g cm^{-3}), an increasing pore size increases the thermal conductivity when the pores are in the range of 1–5 mm. For the largest pores (5 mm diameter), there might be a contribution from convection [110,112]. Few other studies suggested no correlation between pore size and thermal conductivity [73,102]. In Paper IV we performed X-ray microtomography (XMT) analyses of the structure and compared structural data to the thermal conductivity. The pore size data are recalculated into equivalent sphere diameter (D_{eq}) that describes the diameter of a sphere with same volume as the corresponding pore in the sample.

The structure of CRT panel glass foamed using Mn_3O_4 and carbon is shown in Figure 4.6. The glass foam shows a broad range of pores which is confirmed by pore size distributions (Figure 4.7). The limiting factor of the XMT analyses is the resolution of the small pores inside the walls for large samples as the ones investigated here. This is seen by comparing the zoom-in of the XMT image (Figure 4.7b) and the SEM image of the pore walls and struts (Figure 4.7c). This reduces the porosity of the glass foams obtained from XMT image analysis.

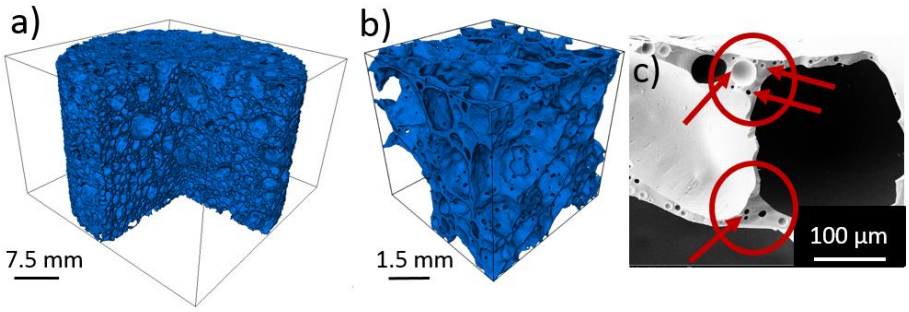

Figure 4.6 3D micrographic reconstructions of the pore structure of glass foams prepared from CRT panel glass, Mn_3O_4 and carbon in a) full-size and b) subvolume. c) SEM image of the struts and pore walls where pores are marked by red arrows. Images are from Paper IV.

The pore size distributions show a majority of small pores (<0.2 mm), however, the gas volume consist mainly of pores larger than 0.5 mm (Figure 4.7b). The same trend is shown in literature [149]. The size distribution varies as four samples exhibit a monomodal distribution (marked will a full line in Figure 4.7a) while three samples have a bimodal distribution (marked with a dashed line in Figure 4.7a).

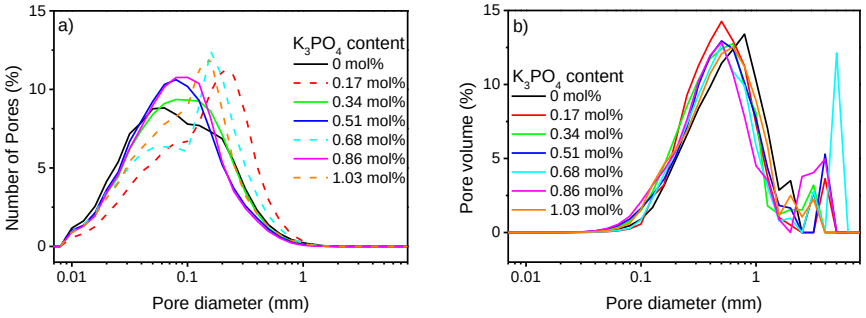

Figure 4.7 Distribution of pore size (based on equivalent sphere diameter) of glass foams with different K_3PO_4 content (XMT data). a) Number of pores and b) pore volume for increasing pore diamter. Figures are from Paper IV.

The wall thickness is analyzed from subvolumes as the one shown in Figure 4.6b. The wall thickness differs among the samples (Figure 4.8). Two samples (K_3PO_4 =0.17 and 0.86 mol%) exhibit much narrower walls (majority <35 µm) than the

remaining samples that show walls as thick as 75–80 µm. The reason for this difference is unknown, but it is not related to the chemical difference of the samples as there is no trend directly correlating to the K_3PO_4 content.

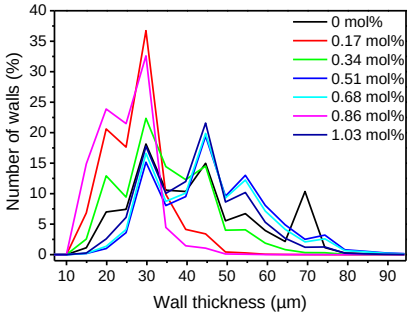

Figure 4.8 Distribution of wall thickness of glass foams prepared from CRT panel glass, Mn_3O_4, and carbon with different K_3PO_4 content (XMT data).

The usual decreasing thermal conductivity with increasing porosity is to some extent found (Figure 4.9). However, two samples (marked as triangles in Figure 4.9) stand out to this trend indicating that the thermal conductivity is more complicated to understand. The porosity range is small (87–89.5 %). Various studies in literature show the same trend with one or more samples standing significantly out from the linear trend [45,78,102]. It is also noted that the chemical difference, i.e., K_3PO_4 addition, has no influence on the thermal conductivity.

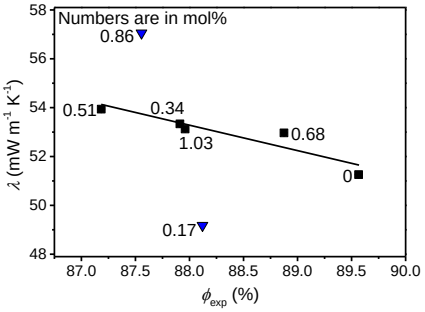

Figure 4.9 Change in thermal conductivity (λ) with the experimental porosity (ϕ_{exp}). The line is a visual guideline. Data marked with triangles are outliers from the linear trend. Figure is from Paper IV.

The pore size shows an effect on the thermal conductivity (Figure 4.10a). The thermal conductivity decreases with increasing average pore size in the range 0.10–0.16 mm. This is in contrast to findings by Köse and Bayer [35] who reported an increasing thermal conductivity with increasing pore size. However, Köse and Bayer report on findings for pores in the range of 1–5 mm which is significantly larger than

the values seen in Figure 4.10a. In contrast to the thermal conductivity, an optimum pore size around 0.13 mm is found for the porosity. The wall thickness does not show any correlation with thermal conductivity or porosity (Figure 4.10b).

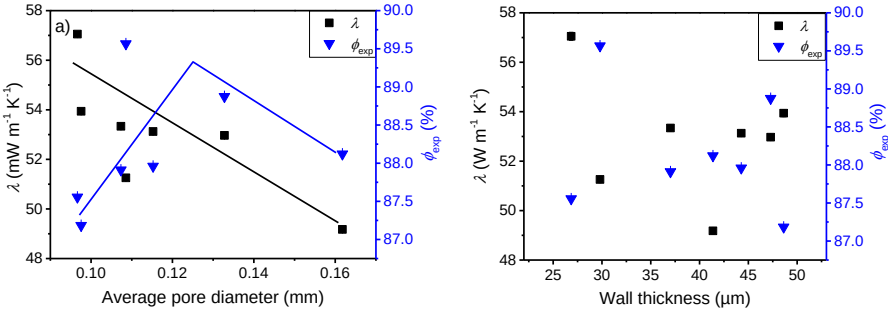

Figure 4.10 Change in thermal conductivity (λ) and experimental porosity (ϕ_{exp}) with a) increasing average pore diameter based on equivalent sphere diameter and b) increasing average wall thickness. The lines are intended as visual guidelines. Figure a) is from Paper IV.

4.5. SUMMARY

Thermal conductivity of glass foams was discussed regarding the effect of change in the solid phase, i.e., amount amorphous and crystal, the gas phase, i.e., gas compositions with different thermal conductivity, and pore structure. The thermal conductivity of the solid phase depends on the amount of foaming agent incorporated into the structure and the amount of crystals left in the glass matrix. The thermal conductivity is found to increase with increasing content of foaming agent incorporated into the glass structure and with increasing crystals content in the glass matrix. Therefore, it is important to minimize the crystal content in glass foams.

The gaseous contribution to the thermal conductivity of glass foams becomes more pronounced at low density (high porosity) as the gas-to-solid ratio increases. Here we find that glass foams with an Ar-CO_2 gas phase show lower thermal conductivity than glass foams with N_2-CO_2 gas phase at densities lower than 0.6 g cm^{-3}. The relative gas contributions of the Ar-rich and N_2-rich gas phases are 22 % and 31 %, respectively, for the glass foams with the lowest density. In literature, glass foams with equal gas and solid contribution is obtained [76] which is ideal for lowering the total thermal conductivity as the thermal conductivity of gases is much lower than that of solids.

The pore size is found to have an influence on the thermal conductivity. An increasing pore size in the range 0.10–0.16 mm shows a decrease in thermal conductivity from 57 to 49 mW m^{-1} K^{-1}. However, in literature [35] the thermal conductivity is found to increase with increasing pore size in the range 1–5 mm. Hence, optimization of the pore structure is still of interest.

CHAPTER 5. GENERAL DISCUSSION AND PERSPECTIVES

Global warming and energy consumption are of great interest to mankind. Questions like *"How can glass be used to combat global warming?"* [128] and *"How can glass be used to reduce energy consumption and eliminate waste?"* [128] is, therefore, interesting and important for glass science and technology. Glass foams can be produced from waste glasses, i.e., eliminating waste and the production costs of new glass. Moreover, glass foams can be used as thermal insulation, i.e., reduce energy consumption from heating as less heat escapes buildings, and thus, glass foams can help combat the global warming. Another question concerns whether glasses can be designed with exceptionally low thermal conductivity [150]. Depending on how low an exceptionally low thermal conductivity is, this might be answered by glass foams. Thermal conductivity of glass foams has been reported as low as 35 mW m^{-1} K^{-1} for a density of 0.160 g cm^{-3} [151] which is unrealistically low as glass foams with a density of 0.131 g cm^{-3} show 42 mW m^{-1} K^{-1} [71] and industrial glass foams have a declared thermal conductivity ≤36 mW m^{-1} K^{-1} for a glass foam with density of 0.100 g cm^{-3} [152]. However, in common for these values is that it is extremely low considering the high thermal conductivity of the glass skeleton. CRT panel glass used in the present studies has a thermal conductivity of 925 mW m^{-1} K^{-1} [73].

Foaming technique

Glass foams can be produced through a variety of methods ranging from sol-gel methods to foaming of a pristine glass or cullet. In the present thesis, waste CRT panel glass was foamed using the chemical approach described in Chapter 2 or the physical approach described in Chapter 3. From an economical and industrial point of view, only the chemical approach is relevant as it is a one-step process compared to the two-step physical approach that requires a high-pressure sintering step before heating. The second heating is similar to that used in the chemical foaming, and thus, the chemical foaming is cheaper. Comparing the two techniques, the foaming initiates at lower temperature when using the physical approach (540–585 °C (see Figure 3.2a)) compared to the chemical approach (700 °C for CRT panel glass and MnO_2 [73], 700–800 °C bottle glass with SiC [33,73], and in Paper II the foaming starts at 640–665 °C for CRT panel glass, Mn_3O_4, carbon, and alkali phosphate mixtures). It is noted that the foaming temperature is defined differently for the two methods. The lower foaming temperature is possibly due to the pre-sintering process that entraps gases at high pressure inside the sintered body. In contrast, during chemical foaming, the glass powder undergoes a sintering process prior to gas release to entrap the gas released by foaming agents. As the foaming is viscosity dependent, it is possible to lower the foaming temperature by substituting CRT panel glass by a glass that sinters at lower temperature. The foaming agent has to be changed as well as it needs to release gas

within a certain viscosity range of the glass that is suggested by Petersen et al. ($10^{3.7}$–10^{6} Pa s) [46] or Scarinci et al. (10^{3}–10^{5} Pa s) [28].

Considering measurements of the maximum size of a glass foam during foaming, it requires a heating microscope or similar method. Heating microscope is only used in a few studies regarding glass foams [33,72] while also used in Paper II and Paper III. The maximum size of a physically foamed glass in Paper III is 600 % of the initial pellet size which is pre-sintered. In Paper II, glass foams expand up to 700 % of a non-sintered pellet. Hence, these undergo a sintering process during heating prior to foaming causing their expansion from the sintered state to be even larger compared to the ones prepared by physical foaming. Petersen et al. [72] report expansion curves for both their own work and work by Bayer and Köse [33]. These expansion curves show expansion up to 1100 % for CRT panel glass and MnO_2 and 900 % for bottle glass and SiC. Based on the expansion, the chemical foaming is advantageous in order to produce low density glass foams.

Thermal conductivity

Thermal conductivity of glass foams generally decreases linearly with increasing porosity (and thus, decreasing density) [30,71,78,102,104,143,153]. However, as seen in Figure 4.9, this is not always that simple and, therefore, the thermal conductivity is more difficult to explain. Petersen [30] investigated the effect of changing the atmosphere from O_2 to CO_2 by the use of different foaming agents. They found no difference in the thermal conductivity and suggested that the effect is minimized due to changes in the solid phase either from incorporation of the foaming agent to the glass or by foaming agent residues as crystals in the glass matrix. A change in thermal conductivity of the solid phase by fully or partly dissolved foaming agents is confirmed by the results shown in Figure 4.3 showing an increase in solid conductivity with increasing MnO_2 or Fe_2O_3 in the solid phase, and a larger increase for samples containing crystal residues. Moreover, König et al. [78] showed that the thermal conductivity decreases linearly with decreasing density for samples prepared with same composition, however, changing the solid composition greatly affects the thermal conductivity. For instance, using same foaming agent content but substituting CRT panel glass by flat glass increases the thermal conductivity by about 20 % [78]. Therefore, the glass composition and foaming agent content greatly affect the thermal conductivity, and thus, the glass composition needs to be optimized while the amount of foaming agents should be minimized.

The impact of gas phase on thermal conductivity is more difficult to investigate as experienced by Petersen [30] due to the impact of, e.g., the solid phase. Therefore, we used the physical approach described in Chapter 3 to obtain samples with similar chemistry. However, we had to assume the pore size to be equal for all glass foams and that the solid phase did not change in order to discuss the gaseous contribution. However, as seen in Paper V, the pore size increases with increasing processing

temperature. The increasing pore size probably causes the decrease in density as suggested in literature [144]. Furthermore, even though CRT panel glass exhibits excellent chemical stability, the samples are found to crystallize slightly due to the repeating heat-treatments (see Paper V). With these variations from the ideal case in mind, the gas phase affects the thermal conductivity of glass foams (Figure 4.5). The theoretical difference in thermal conductivity of the two gas phases is found to be 6.7 mW m^{-1} K^{-1} (Table 4.1). Additionally, as described above König et al. [78] showed a difference in thermal conductivity based on the glass composition. That difference could, though, partly be attributed to changes in the gas phase composition as the CRT panel glass containing foams obtain a higher CO_2 content compared to flat glass containing foams. CO_2 is less thermal conducting than CO, which is reported to be the main secondary gas. The thermal conductivity of the gas phase should be more important when the density decreases. In the present thesis, the gaseous contribution (λ_{gax}/λ) to the thermal conductivity is found to be 22 % for samples with the lowest density. König et al. [76] found the gaseous and solid contribution to be almost equal to the total thermal conductivity. Even with these findings on the gaseous impact on thermal conductivity of glass foams, the exact contribution of the gas phase is not yet fully understood.

In relation to the impact of the gas phase on the thermal conductivity and the results shown in Figure 4.5, the pore size plausibly influences the results. We found that an increase in pore size from 0.10–0.16 mm decreases the thermal conductivity by more than 10 % (see Figure 4.10a). A recent study also suggests that the increasing pore size (covering the range 0.16–2.14 mm) could be the reason that the thermal conductivity decreases for glass foams with similar porosity covering the range 37–84 % [145]. In contrast, for glass foams with pore sizes ranging from 1–5 mm, the thermal conductivity is found to increase with increasing pore size [33]. Finally, two studies find no measurable effect of the pore size on thermal conductivity of glass foams with porosities >85 % [73,102]. With these contradicting studies, the understanding of pore structure is definitely not yet understood. Moreover, the interconnectivity of the pores affects the thermal conductivity as these weakens the porosity effect, and thus, results in a smaller decrease in thermal conductivity [154]. Last, with increasing temperature of the surroundings, the pores should be as small as possible to reduce the total thermal conductivity [155]. A better understanding of this effect could be obtained by producing glass foams with a more narrow size distribution than shown in Figure 4.7. Also, simulation of thermal conductivity through glass foams with different pore structures could give more insight into this field.

Perspectives

For future improvement of the thermal conductivity of glass foams, nanoporosity is suggested in literature [150]. Nanoporous materials such as aerogels exhibit a thermal conductivity of only 15 mW m^{-1} K^{-1} [156]. Based on that, nanoporous glass

foams are expected to show extraordinary insulating properties compared to common insulation materials, and therefore, it is of great interest to work towards such material.

Mechanical properties such as compressive strength are important for glass foams used for building purposes. The CleanTechBlocks that are the overall aim in this project need high strength glass foams as it is a part of a load-bearing wall. The problem with glass foams when reaching for superior mechanical properties is that, e.g., the compressive strength decreases with increasing porosity [63,84,102,104,157,158], hence, the opposite trend than thermal conductivity. Another way of improving the mechanical properties is by introducing crystals as glass-ceramic foams have higher compressive strength than glass foams [67,159], however, this also increases the thermal conductivity. Therefore, it is necessary to optimize the processing to improve the mechanical properties of glass foams without sacrificing the insulating behavior.

As an insulation material it is important that the glass foams exhibit a good chemical durability and do not leach any hazardous compounds. The CRT panel glass is found not to leach any lead [10,160]. However, glass foams prepared from CRT panel glass and SiC or TiN leach barium and strontium. The barium leaching is under the regulatory levels, while the strontium leaching depends on the porosity whether it is above or under the regulatory levels [160]. Therefore, leaching tests are of great interest in the future. Moreover, the chemical durability of the produced glass foams is important. If the glass foams exhibit a poor chemical durability, it might cause dissolution of the outer pore walls creating open pores. Open pores can further be the cause of breakage due to water penetration as water can undergo freeze-thaw cycles. These cycles cause periodic expansion of the volume causing the pore walls to break.

CHAPTER 6. CONCLUSIONS

The present thesis has focused on two main issues: foaming techniques and thermal conductivity of glass foams. We have enhanced the understanding of thermal conductivity of glass foams. Based on this knowledge, optimization of the foaming process in order to tailor the properties of the final glass foams can start.

Foaming of glass is usually achieved by mixing glass powder and a foaming agent, e.g., metal carbonates or transition metal oxides or carbonaceous substances. When heating the mixture above the softening temperature of the glass, it becomes less viscous and the foaming agent either decomposes or chemically reduces or oxidizes when dissolving into the glass structure forming gas. This results in a porous structure that is trapped by cooling. Various types of waste can be added to the powder mixture to either reuse them or improve the foam properties. We investigated the effect of different alkali phosphates on glass foams, as some sodium phosphates were claimed to have a foam stabilizing effect. The results show that neither Li_3PO_4, Na_3PO_4, nor K_3PO_4 show any effect on the porous structure, i.e., pore size, pore shape, or wall thickness, within the tested range of concentration (0-1.03 mol%). Li_3PO_4 and Na_3PO_4 caused foam collapse at high concentrations, i.e., 0.34 mol% and 0.86 mol%, respectively, for the tested temperature program. In contrast, K_3PO_4 showed promising results as additive in order to obtain a high degree of closed pores without compromising the total porosity.

A different approach to produce glass foams is high-pressure sintering. This method involves two steps. First, green bodies of glass powder are sintered under high pressure. Second, the sintered pellets are reheated causing expansion due to the high internal gas pressure in the closed pores and the decreasing viscosity of the glass. We extended the knowledge on using this approach by incorporating different inert gases (He, Ar, and N_2) at various pressures (5–25 MPa). The foaming onset, maximum expansion, and final foam characteristics depend greatly on the size of the gas specie and sintering pressure. We found that the foaming initiates at lower temperature with decreasing kinetic diameter of the gas and increasing pressure. The maximum expansion increases with increasing kinetic diameter. Similar correlations are found for foam characteristics as porosity. In contrast, the pressure dependence show a maximum at 20 MPa giving the largest foaming and highest porosity. Additionally, it is verified by gas analysis that the sintering gas is entrapped in the glass foam (only Ar and N_2 are measured), though, with high concentrations of CO_2 due to impurities from the experimental setup. The CO_2 development is suggested to aid the foaming of the glass foams.

The solid phase, gas phase, and macrostructure of glass foams or glass foam systems were analyzed and their relation to the thermal conductivity was described. The thermal conductivity increases with increasing content of foaming agent (Fe_2O_3

and MnO_2) added to the CRT panel glass. The increase is both found for melt-quenched samples where the foaming agent is fully incorporated into the glass structure, and for sintered samples where the foaming agent is partly incorporated and partly embedded in the glassy matrix. Moreover, the crystal containing samples show a higher thermal conductivity due to a higher thermal conductivity of crystals compared to glasses. Therefore, it is crucial to minimize the crystal content by having the foaming agents fully dissolved in the glass structure. For this purpose, the temperature program needs to be optimized to secure a high dissolution rate while maintaining a highly porous glass melt without foam collapse. Additionally, the amount of foaming agents should also be limited in order to keep the solid conductance as low as possible.

The gas phase of glass foams is difficult to control. We used a physical foaming approach in order to try to control the chemistry of the solid and gas phase. Ar and N_2 was entrapped in the glass foams. Impurities (carbon) from the experimental setup caused binary gas mixtures with the sintering gas (Ar or N_2) and CO_2 due to oxidation of the carbon particles. Theoretical calculations on the thermal conductivity of the gas mixtures were used to determine the difference between the gas compositions. All Ar-sintered samples show the same thermal conductivity, and the same tendency is found for all N_2-sintered samples. However, the thermal conductivity of the Ar containing gas phases were found to be 6.7 mW m^{-1} K^{-1} lower than the N_2 containing ones. This is caused by the lower thermal conductivity of Ar compared to N_2. The lower gas thermal conductivity causes a lower thermal conductivity of the glass foams. Therefore, it is important to tailor the gas composition to contain low thermal conducting gases such as CO_2 to lower the total thermal conductivity of glass foams.

The pore size of glass foams should be determined with caution because of a broad size distribution. The pore walls contain pores in the µm-range while the largest pores can be in the mm-range. We analyzed the pore sizes and wall thicknesses of seven glass foams and found no correlation between wall thickness and thermal conductivity of glass foams. On the contrary, the thermal conductivity decreases by >10 % when the average pore size increases from 0.10 mm to 0.16 mm.

In general, we find that the chemical foaming results in a larger foaming than the physical foaming approach, i.e., the chemical foaming is preferred in order to obtain highly porous glass foams which exhibit a lower thermal conductivity. The glass foams should be prepared with carbonaceous substances in order to entrap CO_2 in the pores, while the foaming agents should be fully dissolved in the glass matrix as these two parameters will decrease the total thermal conductivity of the glass foams.

BIBLIOGRAPHY

[1] A.M. Papadopoulos, State of the art in thermal insulation materials and aims for future developments, Energy Build. 37 (2005) 77–86.

[2] B.P. Jelle, Traditional, state-of-the-art and future thermal building insulation materials and solutions - Properties, requirements and possibilities, Energy Build. 43 (2011) 2549–2563.

[3] A. Karamanos, S. Hadiarakou, A.M. Papadopoulos, The impact of temperature and moisture on the thermal performance of stone wool, Energy Build. 40 (2008) 1402–1411.

[4] F. Domínguez-Muñoz, B. Anderson, J.M. Cejudo-López, A. Carrillo-Andrés, Uncertainty in the thermal conductivity of insulation materials, Energy Build. 42 (2010) 2159–2168.

[5] J. Fricke, U. Heinemann, H.P. Ebert, Vacuum insulation panels-From research to market, Vacuum. 82 (2008) 680–690.

[6] Z. Yao, T.-C.C. Ling, P.K.K. Sarker, W. Su, J. Liu, W. Wu, J. Tang, Recycling difficult-to-treat e-waste cathode-ray-tube glass as construction and building materials: A critical review, Renew. Sustain. Energy Rev. 81 (2018) 595–604.

[7] L. Rocchetti, F. Beolchini, Environmental burdens in the management of end-of-life cathode ray tubes, Waste Manag. 34 (2014) 468–474.

[8] F. Méar, P. Yot, M. Ribes, Effects of temperature, reaction time and reducing agent content on the synthesis of macroporous foam glasses from waste funnel glasses, Mater. Lett. 60 (2006) 929–934.

[9] F. Méar, P. Yot, M. Cambon, M. Ribes, The characterization of waste cathode-ray tube glass, Waste Manag. 26 (2006) 1468–1476.

[10] S.E. Musson, Y.C. Jang, T.G. Townsend, I.H. Chung, Characterization of lead leachability from cathode ray tubes using the Toxicity Characteristic Leaching Procedure, Environ. Sci. Technol. 34 (2000) 4376–4381.

[11] C. Zhang, J. Wang, J. Bai, J. Guan, W. Wu, C. Guo, Recovering lead from cathode ray tube funnel glass by mechano-chemical extraction in alkaline solution, Waste Manag. Res. 31 (2013) 759–763.

[12] M. Chen, F.-S. Zhang, J. Zhu, Lead recovery and the feasibility of foam glass

production from funnel glass of dismantled cathode ray tube through pyrovacuum process, J. Hazard. Mater. 161 (2009) 1109–1113.

[13] H.-Y. Kang, J.M. Schoenung, Electronic waste recycling: A review of U.S. infrastructure and technology options, Resour. Conserv. Recycl. 45 (2005) 368–400.

[14] J.R. Mueller, M.W. Boehm, C. Drummond, Direction of CRT waste glass processing: Electronics recycling industry communication, Waste Manag. 32 (2012) 1560–1565.

[15] M. Limbachiya, M.S. Meddah, S. Fotiadou, Performance of granulated foam glass concrete, Constr. Build. Mater. 28 (2012) 759–768.

[16] A. Arulrajah, M.M. Disfani, F. Maghoolpilehrood, S. Horpibulsuk, A. Udonchai, M. Imteaz, Y.J. Du, Engineering and environmental properties of foamed recycled glass as a lightweight engineering material, J. Clean. Prod. 94 (2015) 369–375.

[17] P. Colombo, G. Brusatin, E. Bernardo, G. Scarinci, Inertization and Reuse of Waste Materials by Vitrification and Fabrication of Inertization and reuse of waste materials by vitrification and fabrication of glass-based products, Curr. Opin. Solid State Mater. Sci. 7 (2003) 336–239.

[18] Pittsburgh Corning Europe, Foamglas industrial insulation handbook, Pittsburgh Corning Europe, 1992.

[19] R.G.C. Beerkens, J. van der Schaaf, Gas Release and Foam Formation During Melting and Fining of Glass, J. Am. Ceram. Soc. 89 (2006) 24–35.

[20] D. Kim, P. Hima, Foaming in Glass Melts Produced by Sodium Sulfate Decomposition under Isothermal Conditions, J. Am. Ceram. Soc. 74 (1991) 551–555.

[21] J. Van Der Schaaf, R.G.C. Beerkens, A model for foam formation , stability , and breakdown in glass-melting furnaces, J. Colloid Interface Sci. 295 (2006) 218–229.

[22] M.J. Varady, A.G. Fedorov, Combined Radiation and Conduction in Glass Foams, J. Heat Transf. 124 (2002) 1103-.

[23] A.G. Fedorov, L. Pilon, Glass foams: Formation, transport properties, and heat, mass, and radiation transfer, J. Non. Cryst. Solids. 311 (2002) 154–173.

[24] P. Hrma, Effect of heating rate on glass foaming: Transition to bulk foam, J. Non. Cryst. Solids. 355 (2009) 257–263.

[25] F. Pigeonneau, H. Kočárková, F. Rouyer, Stability of vertical films of molten glass due to evaporation, Colloids Surfaces A Physicochem. Eng. Asp. 408 (2012) 8–16.

[26] M. Jensen, Y. Yue, R. Keding, Effect of Bubbles on the Characterisation of Striae in Glasses Bubble formation in basalt-like melts, Glas. Technol. Eur. J. Glas. Sci. Technol. A. 52 (2011) 127–135.

[27] B. Long, Glass product and method of manufacturing sponge-like glass, US Patent 1,945,052, 1934.

[28] G. Scarinci, G. Brusatin, E. Bernardo, Glass foams, in: M. Scheffler, P. Colombo (Eds.), Cell. Ceram. Struct. Manuf. Prop. Appl., Wiley-VCH Verlag GmbH & Co KGaA, Weinheim, 2005: pp. 158–176.

[29] L. Kern, Process of manufacturing porous silica ware, US Patent 1,898,839, 1933.

[30] R.R. Petersen, Foam Glass for Construction Materials: Foaming Mechanism and Thermal Conductivity, Aalborg University (PhD Thesis), 2015.

[31] J.D. Mackenzie, Foamed glass and tiles from waste containers, in: Symp. Util. Waste Glas. Second. Prod., Technology Application Center, 1973: p. 291.

[32] B.D. Marchant, I.B. Cutler, Foamed glass insulation from waste glass, in: Symp. Util. Waste Glas. Second. Prod., Technology Application Center, 1973: p. 277.

[33] G. Bayer, S. Köse, Reaction of foaming additives with waste glass powders in the preparation of lightweight materials, Riv. Della Stn. Sper. Del Vetro. 9 (1979) 310–320.

[34] G. Bayer, Foaming of borosilicate glasses by chemical reactions in the temperature range 950 - 1150°C, J. Non. Cryst. Solids. 39 (1980) 855–860.

[35] S. Köse, G. Bayer, Schaumbildung im system altglas-SiC und die eigenschaften derartiger schaumgläser, Glas. Ber. 55 (1982) 151–160.

[36] V. Ducman, M. Kovacevic, The foaming of waste glass, Key Eng. Mater. 132–136 (1997) 2264–2267.

[37] I. Brusatin, G. Lancellotti, L. Scarinci, G. Barbieri, P. Colombo, Glass cullet: scrap or new raw material?, in: R.K. Dhir, M.C. Limbachiya, T.D. Dyer (Eds.), Recycl. Reuse Glas. Cullet Proc. Int. Symp. Organised by Concr. Technol. Unit Held Univ. Dundee, Scotland, UK 19-20 March 2001, Thomas Telford Books, 2001: pp. 93–102.

[38] G. Brusatin, E. Bernardo, G. Scarinci, Production of Foam Glass from Glass Waste, in: L.M. Limbachiya, J.J. Roberts (Eds.), Sustain. Waste Manag. Recycl. Proc. Int. Conf. Organ. by Concr. Mason. Res. Kingst. Univ. London, Thomas Telford Publishing, London, UK, 2004: pp. 67–82.

[39] M.W. Kearns, Formation of porous bodies, US Patent 4,659,546, 1987.

[40] N.G.D. Murray, D.C. Dunand, Effect of thermal history on the superplastic expansion of argon-filled pores in titanium : Part I kinetics and microstructure, Acta Mater. 52 (2004) 2269–2278.

[41] P. Sepulveda, J.R. Jones, L.L. Hench, Bioactive sol-gel foams for tissue repair, J. Biomed. Mater. Res. 59 (2002) 340–348.

[42] R. Gupta, A. Kumar, Bioactive materials for biomedical applications using sol-gel technology, Biomed. Mater. 3 (2008) 034005.

[43] J.R. Jones, L.M. Ehrenfried, L.L. Hench, Optimising bioactive glass scaffolds for bone tissue engineering, Biomaterials. 27 (2006) 964–973.

[44] G. Kyaw, O. D 'amore, M. Caniato, A. Travan, G. Turco, L. Marsich, A. Ferluga, C. Schmid, An innovative acoustic insulation foam from recycled waste glass powder, J. Clean. Prod. 165 (2017) 1306–1315.

[45] J. König, R.R. Petersen, Y. Yue, Influence of the glass particle size on the foaming process and physical characteristics of foam glasses, J. Non. Cryst. Solids. 447 (2016) 190–197.

[46] R.R. Petersen, J. König, Y. Yue, The viscosity window of the silicate glass foam production, J. Non. Cryst. Solids. 456 (2017) 49–54.

[47] B. Chen, K. Wang, X. Chen, A. Lu, Study of foam glass with high content of fly ash using calcium carbonate as foaming agent, Mater. Lett. 79 (2012) 263–265.

[48] J. König, R.R. Petersen, Y. Yue, Influence of the glass–calcium carbonate mixture's characteristics on the foaming process and the properties of the foam glass, J. Eur. Ceram. Soc. 34 (2014) 1591–1598.

[49] B. Tang, J. Lin, S. Qian, J. Wang, S. Zhang, Preparation of glass-ceramic foams from the municipal solid waste slag produced by plasma gasification process, Mater. Lett. 128 (2014) 68–70.

[50] C. Mugoni, M. Montorsi, C. Siligardi, F. Andreola, I. Lancellotti, E. Bernardo, L. Barbieri, Design of glass foams with low environmental impact, Ceram. Int. 41 (2015) 3400–3408.

[51] E. Bernardo, F. Albertini, Glass foams from dismantled cathode ray tubes, Ceram. Int. 32 (2006) 603–608.

[52] E. Bernardo, G. Scarinci, S. Hreglich, Foam glass as a way of recycling glasses from cathode ray tubes, Glas. Sci. Technol. 78 (2005) 7–11.

[53] C.T. Lee, Production of alumino-borosilicate foamed glass body from waste LCD glass, J. Ind. Eng. Chem. 19 (2013) 1916–1925.

[54] N.M.P. Low, Formation of cellular-structure glass with carbonate compounds and natural mica powders, J. Mater. Sci. 16 (1981) 800–808.

[55] Z. Matamoros-Veloza, J.C. Rendón-Angeles, K. Yanagisawa, E.E. Mejia-Martínez, J.R. Parga, Low temperature preparation of porous materials from TV panel glass compacted via hydrothermal hot pressing, Ceram. Int. 41 (2015) 12700–12709.

[56] R.R. Petersen, J. König, M.M. Smedskjaer, Y. Yue, Foaming of CRT panel glass powder using Na_2CO_3, Glas. Technol. Eur. J. Glas. Sci. Technol. A. 55 (2014) 1–6.

[57] R.R. Petersen, J. König, M.M. Smedskjaer, Y. Yue, Effect of Na_2CO_3 as foaming agent on dynamics and structure of foam glass melts, J. Non. Cryst. Solids. 400 (2014) 1–5.

[58] W. Gene Ramsey, Acoustic driven toughened foam glass abrasive devices and a method for producing the same, US Patent 20080190036A1, 2008.

[59] H.R. Fernandes, D.D. Ferreira, F. Andreola, I. Lancellotti, L. Barbieri, J.M.F. Ferreira, Environmental friendly management of CRT glass by foaming with waste egg shells, calcite or dolomite, Ceram. Int. 40 (2014) 13371–13379.

[60] H.R. Fernandes, D.U. Tulyaganov, J.M.F. Ferreira, Preparation and characterization of foams from sheet glass and fly ash using carbonates as foaming agents, Ceram. Int. 35 (2009) 229–235.

[61] A. Pokorny, J. Vicenzi, C. Pérez Bergmann, Influence of heating rate on the microstructure of glass foams., Waste Manag. Res. 29 (2011) 172–179.

[62] H.R. Fernandes, F. Andreola, L. Barbieri, I. Lancellotti, M.J. Pascual, J.M.F. Ferreira, The use of egg shells to produce Cathode Ray Tube (CRT) glass foams, Ceram. Int. 39 (2013) 9071–9078.

[63] M.T. Souza, B.G.O. Maia, L.B. Teixeira, K.G. de Oliveira, A.H.B. Teixeira, A.P. Novaes de Oliveira, Glass foams produced from glass bottles and eggshell wastes, Process Saf. Environ. Prot. 111 (2017) 60–64.

[64] L.B. Teixeira, V.K. Fernandes, B.G.O. Maia, S. Arcaro, A.P.N. de Oliveira, Vitrocrystalline foams produced from glass and oyster shell wastes, Ceram. Int. 43 (2017) 6730–6737.

[65] M.S. Heydari, S.M. Mirkazemi, S. Abbasi, Influence of Co_3O_4, Fe_2O_3 and SiC on microstructure and properties of glass foam from waste cathode ray tube display panel (CRT), Adv. Appl. Ceram. 113 (2014) 234–239.

[66] X. Wang, D. Feng, B. Zhang, Z. Li, C. Li, Y. Zhu, Effect of KNO3 on the microstruture and physical properties of glass foam from solid waste glass and SiC powder, Mater. Lett. 169 (2016) 21–23.

[67] H.W. Guo, Y.X. Gong, S.Y. Gao, Preparation of high strength foam glass-ceramics from waste cathode ray tube, Mater. Lett. 64 (2010) 997–999.

[68] E. Bernardo, R. Cedro, M. Florean, S. Hreglich, Reutilization and stabilization of wastes by the production of glass foams, Ceram. Int. 33 (2007) 963–968.

[69] S. Abbasi, S.M. Mirkazemi, A. Ziaee, M. Saeedi Heydari, The effects of Fe_2O_3 and Co_3O_4 on microstructure and properties of foam glass from soda lime waste glasses, Glas. Phys. Chem. 40 (2014) 173–179.

[70] V. Ducman, L. Korat, A. Legat, B. Mirtič, X-ray micro-tomography investigation of the foaming process in the system of waste glass-silica mud-MnO_2, Mater. Charact. 86 (2013) 316–321.

[71] J. König, R.R. Petersen, Y. Yue, Fabrication of highly insulating foam glass made from CRT panel glass, Ceram. Int. 41 (2015) 9793–9800.

[72] R.R. Petersen, J. König, Y. Yue, Evaluation of foaming behavior of glass melts by high-temperature microscopy, Int. J. Appl. Glas. Sci. (2016) 1–8.

[73] R.R. Petersen, J. König, Y. Yue, The mechanism of foaming and thermal

conductivity of glasses foamed with MnO_2, J. Non. Cryst. Solids. 425 (2015) 74–82.

[74] A.S. Llaudis, M.J.O. Tari, F.J.G. Ten, E. Bernardo, P. Colombo, Foaming of flat glass cullet using Si_3N_4 and MnO_2 powders, Ceram. Int. 35 (2009) 1953–1959.

[75] J. König, R.R. Petersen, Y. Yue, D. Suvorov, Gas-releasing reactions in foam-glass formation using carbon and Mn_xO_y as the foaming agents, Ceram. Int. 43 (2017) 4638–4646.

[76] J. König, V. Nemanič, M. Žumer, R.R. Petersen, M.B. Østergaard, Y. Yue, D. Suvorov, Evaluation of the contributions to the effective thermal conductivity of an open-porous type foam glass, Constr. Build. Mater. (2019).

[77] R.R. Petersen, J. König, N. Iversen, M.B. Østergaard, Y. Yue, The foaming mechanism of glass foams prepared from Mn_3O_4, carbon and CRT panel glass, (2019).

[78] J. König, R.R. Petersen, N. Iversen, Y. Yue, Suppressing the effect of cullet composition on the formation and properties of foamed glass, Ceram. Int. 44 (2018) 11143–11150.

[79] V. Laur, R. Benzerga, R. Lebullenger, L. Le Gendre, G. Lanoë, A. Sharaiha, P. Queffelec, Green foams for microwave absorbing applications: Synthesis and characterization, Mater. Res. Bull. 96 (2017) 100–106.

[80] C.F. Cooper, J.A. Kitchener, The foaming of molten silicates, J. Iron Steel Inst. 193 (1959) 48–55.

[81] C.H. Chen, K.Q. Feng, Y. Zhou, H.L. Zhou, Effect of sintering temperature on the microstructure and properties of foamed glass-ceramics prepared from high-titanium blast furnace slag and waste glass, Int. J. Miner. Metall. Mater. 24 (2017) 931–936.

[82] L. Ding, W. Ning, Q. Wang, D. Shi, L. Luo, Preparation and characterization of glass–ceramic foams from blast furnace slag and waste glass, Mater. Lett. 141 (2015) 327–329.

[83] H. Wang, K. Feng, Y. Zhou, Q. Sun, H. Shi, Effects of $Na_2B_4O_7{\cdot}5H_2O$ on the properties of foam glass from waste glass and titania-bearing blast furnace slag, Mater. Lett. 132 (2014) 176–178.

[84] Y. Guo, Y. Zhang, H. Huang, P. Hu, Effect of heat treatment process on the

preparation of foamed glass ceramic from red mud and fly ash, Appl. Mech. Mater. 670 (2014) 201–204.

[85] C. Zhai, Z. Li, Y. Zhu, J. Zhang, X. Wang, L. Zhao, L. Pan, P. Wang, Effects of Sb_2O_3 on the mechanical properties of the borosilicate foam glasses sintered at low temperature, Adv. Mater. Sci. Eng. 2014 (2014).

[86] J.E. Shelby, Introduction to glass science and technology, 2nd ed., The royal society of chemistry, 2005.

[87] A. Jambon, J.P. Carron, Diffusion of Na, K, Rb and Cs in glasses of albite and orthoclase composition, Geochim. Cosmochim. Acta. 40 (1976) 897–903.

[88] B.O. Mysen, P. Richet, Silicate glasses and melts: properties and structure, 1st ed., Elsevier, 2005.

[89] Y. Yue, R. Brückner, Influence of homologous substitutions of chemical composition on the rheological properties and on isochomal workability of silicate glass melts, Glas. Sci. Technol. 69 (1996) 204–215.

[90] J. Kjeldsen, M.M. Smedskjaer, J.C. Mauro, Y. Yue, On the origin of the mixed alkali effect on indentation in silicate glasses, J. Non. Cryst. Solids. 406 (2014) 22–26.

[91] A. Kucuk, A.G. Clare, L. Jones, An estimation of the surface tension for silicate glass melts at 1400°C using statistical analysis, Glas. Technol. 40 (1999) 149–153.

[92] D.T. Queheillalt, K.A. Gable, H.N.G. Wadley, Temperature dependent creep expansion of Ti-6Al-4V low density core sandwich structures, Scr. Mater. 44 (2001) 409–414.

[93] S. Oppenheimer, D.C. Dunand, Solid-state foaming of Ti–6Al–4V by creep or superplastic expansion of argon-filled pores, Acta Mater. 58 (2010) 4387–4397.

[94] B. Wang, K. Matsumaru, J. Yang, Z. Fu, K. Ishizaki, Mechanical behavior of cellular borosilicate glass with pressurized Ar-filled closed pores, Acta Mater. 60 (2012) 4185–4193.

[95] G. Shen, Q. Mei, V.B. Prakapenka, P. Lazor, S. Sinogeikin, Y. Meng, C. Park, Effect of helium on structure and compression behavior of SiO_2 glass, Proc. Natl. Acad. Sci. 108 (2011) 6004–6007.

[96] D.P. Broom, Techniques for the measurement of gas adsorption by carbon nanostructures, in: M.L. Terranova, S. Orlanducci, M. Rossi (Eds.), Carbon Nanomater. Gas Adsorpt., 2012: pp. 1–38.

[97] T. Sato, N. Funamori, T. Yagi, Helium penetrates into silica glass and reduces its compressibility, Nat. Commun. 2 (2011) 345.

[98] F.J. Norton, Helium Diffusion Through Glass, J. Am. Ceram. Soc. 36 (1953) 90–96.

[99] C. Weigel, A. Polian, M. Kint, B. Rufflé, M. Foret, R. Vacher, Vitreous silica distends in helium gas: Acoustic versus static compressibilities, Phys. Rev. Lett. 109 (2012) 1–5.

[100] C. Weigel, M. Foret, B. Hehlen, M. Kint, S. Clément, A. Polian, R. Vacher, B. Rufflé, Polarized raman spectroscopy of v-SiO_2 under rare-gas compression, Phys. Rev. B. 93 (2016) 1–9.

[101] D.C. Jana, G. Sundararajan, K. Chattopadhyay, Effect of porosity on structure, Young's modulus, and thermal conductivity of SiC foams by direct foaming and gelcasting, J. Am. Ceram. Soc. 100 (2017) 312–322.

[102] J.P. Wu, A.R. Boccaccini, P.D. Lee, R.D. Rawlings, Thermal and mechanical properties of a foamed glass-ceramic material produced from silicate wastes, Proc. Eighth Eur. Soc. Glas. Sci. Technol. Conf. Glas. Technol. Eur. J. Glas. Sci. Technol. A. 48 (2007) 133–141.

[103] Y. Attila, M. Güden, A. Taşdemirci, Foam glass processing using a polishing glass powder residue, Ceram. Int. 39 (2013) 5869–5877.

[104] F. Méar, P. Yot, R. Viennois, M. Ribes, Mechanical behaviour and thermal and electrical properties of foam glass, Ceram. Int. 33 (2007) 543–550.

[105] C. Vancea, I. Lazău, Glass foam from window panes and bottle glass wastes, Cent. Eur. J. Chem. 12 (2014) 804–811.

[106] E.G. de Moraes, M. Bigi, N.P. Stochero, S. Arcaro, C. Siligardi, A.P. Novaes de Oliveira, Vitrocrystalline foams produced with EPS as pore former: Processing and characterization, Process Saf. Environ. Prot. 121 (2019) 12–19.

[107] K. Swimm, S. Vidi, G. Reichenauer, H.P. Ebert, Coupling of gaseous and solid thermal conduction in porous solids, J. Non. Cryst. Solids. 456 (2017) 114–124.

[108] J.J. Zhao, Y.Y. Duan, X.D. Wang, B.X. Wang, Effects of solid-gas coupling and pore and particle microstructures on the effective gaseous thermal conductivity in aerogels, J. Nanoparticle Res. 14 (2012) 1024.

[109] B.K. Larkin, S.W. Churchill, Heat transfer by radiation through porous insulations, AIChE J. 5 (1959) 467–474.

[110] R.E. Skochdopole, The thermal conductivity of foamed plastics, Chem. Eng. Prog. 57 (1961) 55–59.

[111] E. Placido, M.C. Arduini-Schuster, J. Kuhn, Thermal properties predictive model for insulating foams, Infrared Phys. Technol. 46 (2005) 219–231.

[112] P. Collishaw, J.R.G. Evans, Review An assessment of expressions for the apparent thermal conductivity of cellular materials, J. Mater. Sci. 29 (1994) 2261–2273.

[113] M.K. Choudhary, B. Purnode, A.M. Lankhorst, A.F.J.A. Habraken, Radiative heat transfer in processing of glass-forming melts, Int. J. Appl. Glas. Sci. 9 (2018) 218–234.

[114] R.G. Griskey, Radiation heat transfer, in: Transp. Phenom. Unit Oper. A Comb. Approach, Wiley-Interscience, 2002: pp. 208–227.

[115] E. Solórzano, M.A. Rodriguez-Perez, J. Lazaro, J.A. De Saja, Influence of solid phase conductivity and cellular structure on the heat transfer mechanisms of cellular materials: Diverse case studies, Adv. Eng. Mater. 11 (2009) 818–824.

[116] M. Bouquerel, T. Duforestel, D. Baillis, G. Rusaouen, Heat transfer modeling in vacuum insulation panels containing nanoporous silicas — A review, Energy Build. 54 (2012) 320–336.

[117] B. Nait-Ali, K. Haberko, H. Vesteghem, J. Absi, D.S. Smith, Thermal conductivity of highly porous zirconia, J. Eur. Ceram. Soc. 26 (2006) 3567–3574.

[118] L.W. Hrubesh, R.W. Pekala, Thermal properties of organic and inorganic aerogels, J. Mater. Res. 9 (1994) 731–738.

[119] B. Notario, J. Pinto, E. Solorzano, J.A. De Saja, M. Dumon, M.A. Rodríguez-Pérez, Experimental validation of the Knudsen effect in nanocellular polymeric foams, Polymer (Guildf). 56 (2015) 57–67.

[120] E. Litovsky, M. Shapiro, A. Shavit, Gas pressure and temperature dependences of thermal conductivity of porous ceramic materials: Part 2, refractories and ceramics with porosity exceeding 30%, J. Am. Ceram. Soc. 79 (1996) 1366–76.

[121] E.Y. Litovsky, M. Shapiro, Gas Pressure and Temperature Dependences of Thermal Conductivity of Porous Ceramic Materials: Part 1, Refractories and Ceramics with Porosity below 30%, J. Am. Ceram. Soc. 75 (1992) 3425–39.

[122] K. Swimm, G. Reichenauer, S. Vidi, H.-P. Ebert, Gas Pressure Dependence of the Heat Transport in Porous Solids with Pores Smaller than 10 μm, Int. J. Thermophys. 30 (2009) 1329–1342.

[123] C. Bi, G.H. Tang, Z.J. Hu, H.L. Yang, J.N. Li, Coupling model for heat transfer between solid and gas phases in aerogel and experimental investigation, Int. J. Heat Mass Transf. 79 (2014) 126–136.

[124] J.P. Wu, A.R. Boccaccini, P.D. Lee, M.J. Kershaw, R.D. Rawlings, Glass ceramic foams from coal ash and waste glass : production and characterisation, Adv. Appl. Ceram. 105 (2006) 32–39.

[125] C. Kittel, Interpretation of the Thermal Conductivity of Glasses, Phys. Rev. 755 (1949) 972–974.

[126] N.A. Ghoneim, A.A. Ahmed, S. Gharib, Effect of transition metal conductivity of glass oxides on the thermal conductivity of glass, Thermochim. Acta. 71 (1983) 43–51.

[127] S.N. Salama, S.M. Salman, S. Gharib, Thermal conductivity of some silicate glasses and their respective crystalline products, J. Non. Cryst. Solids. 93 (1987) 203–214.

[128] J.C. Mauro, E.D. Zanotto, Two Centuries of Glass Research: Historical Trends, Current Status, and Grand Challenges for the Future, Int. J. Appl. Glas. Sci. 5 (2014) 313–327.

[129] S.M. Salman, S. Gharib, Thermal conductivity of some multicomponent silicate glasses, Thermochim. Acta. 77 (1984) 227–239.

[130] S.M. Salman, S. Gharib, Some physical properties concerning the thermal conductivity data of BaO-containing silicate glasses in relation to structure, Thermochim. Acta. 82 (1984) 345–355.

[131] P.F. van Velden, Thermal conductivities of some lead and bismuth glasses,

Glas. Technol. 4 (1965) 113–128.

[132] M.K. Choudhary, R.M. Potter, Heat transfer in glass-forming melts, in: L.D. Pye, A. Montenero, I. Joseph (Eds.), Prop. Glas. Melts, Second, CRC Press, Taylor & Francis, 2005.

[133] E. Bernardo, G. Scarinci, P. Bertuzzi, P. Ercole, L. Ramon, Recycling of waste glasses into partially crystallized glass foams, J. Porous Mater. 17 (2010) 359–365.

[134] F. Andreola, L. Barbieri, A. Corradi, I. Lancellotti, R. Falcone, S. Hreglich, Glass-ceramics obtained by the recycling of end of life cathode ray tubes glasses, Waste Manag. 25 (2005) 183–189.

[135] D.S. Smith, A. Alzina, J. Bourret, B. Nait-Ali, F. Pennec, N. Tessier-Doyen, K. Otsu, H. Matsubara, P. Elser, U.T. Gonzenbach, Thermal conductivity of porous materials, J. Mater. Res. 28 (2013) 2260–2272.

[136] D.P.H. Hasselman, L.F. Johnson, Effective Thermal Conductivity of Composites with Interfacial Thermal Barrier Resistance, J. Compos. Mater. 21 (1987) 508–515.

[137] D.P.H. Hasselman, K.Y. Donaldson, J.R.T. Jr, J.J. Brennan, Thermal conductivity of vapor-liquid-solid and vapor-solid silicon carbide whisker-reinforced lithium aluminosilicate glass-ceramic composites, J. Am. Ceram. Soc. 79 (1996) 742–748.

[138] D.P.H. Hasselman, K.Y. Donaldson, J. Liu, L.J. Gauckler, P.D. Ownby, Thermal Conductivity of a particulate-diamond-reinforced cordierite matrix composite, J. Am. Ceram. Soc. 77 (1994) 1757–60.

[139] P.G. Klemens, Thermal Conductivity of Composites, Int. J. Thermophys. 11 (1990) 971–976.

[140] Y. Hiroshima, Y. Hamamoto, S. Yoshida, J. Matsuoka, Thermal conductivity of mixed alkali silicate glasses at low temperature, J. Non. Cryst. Solids. 354 (2008) 341–344.

[141] A. Wassiljewa, Heat conduction in gaseous mixtures, Phys. Z. 5 (1904) 737–742.

[142] M. Yorizane, S. Yoshimura, H. Masuoka, H. Yoshida, Thermal conductivities of binary gas mixtures at high pressures: nitrogen-oxygen, nitrogen-argon, carbon dioxide-argon, and carbon dioxide-methane, Ind. Eng. Chem.

Fundam. 22 (1983) 458–463.

[143] A.R.J. Barbosa, A.A.S. Lopes, S.I.H. Sequeira, J.P. Oliveira, A. Davarpanah, F. Mohseni, V.S. Amaral, R.C.C. Monteiro, Effect of processing conditions on the properties of recycled cathode ray tube glass foams, J. Porous Mater. 23 (2016) 1663–1669.

[144] P. Colombo, J.R. Hellmann, Ceramic foams from preceramic polymers, Mater. Res. Innov. 6 (2002) 260–272.

[145] P.A.M. dos Santos, A.V. Priebbnow, S. Arcaro, R.M. da Silva, D.A.R. Lopez, A.D.A.L. Rodriguez, Sustainable Glass Foams Produced from Glass Bottles and Tobacco Residue, Mater. Res. 22 (2019) e2180452.

[146] A. Michels, J. V Sengers, L.J.M. Van De Klundert, The thermal conductivity of argon at elevated densities, Physica. 29 (1963) 149–160.

[147] A. Michels, J. V Sengers, P.S. van der Gulik, The thermal conductivity of carbon dioxide in the critical region, Physica. 28 (1962) 1216–1237.

[148] A. Michels, A. Botzen, The thermal conductivity of nitrogen at pressures up to 2500 atmospheres, Physica. 19 (1956) 585–598.

[149] L. Korat, V. Ducman, A. Legat, B. Mirtič, Characterisation of the pore-forming process in lightweight aggregate based on silica sludge by means of X-ray micro-tomography (micro-CT) and mercury intrusion porosimetry (MIP), Ceram. Int. 39 (2013) 6997–7005.

[150] J.C. Mauro, C.S. Philip, D.J. Vaughn, M.S. Pambianchi, Glass science in the United States: Current status and future directions, Int. J. Appl. Glas. Sci. 5 (2014) 2–15.

[151] A.A. Ketov, An experience of reuse of a glass cullet for production of foam structure material, in: R.K. Dhir, M.C. Limbachiya, T.D. Dyer (Eds.), Recycl. Reuse Glas. Cullet Proc. Int. Symp. Organised by Concr. Technol. Unit Held Univ. Dundee, Scotland, UK 19-20 March 2001, Thomas Telford Publishing, 2001: p. 85.

[152] Www.foamglass.co.uk, FOAMGLAS® T3+, (2017). https://uk.foamglas.com/en-gb/products/product-overview/foamglas-slabs/foamglas-t3 (accessed January 11, 2019).

[153] C. Bai, T. Ni, Q. Wang, H. Li, P. Colombo, Porosity, mechanical and insulating properties of geopolymer foams using vegetable oil as the

stabilizing agent, J. Eur. Ceram. Soc. 38 (2018) 799–805.

[154] C. Bai, H. Li, E. Bernardo, P. Colombo, Waste-to-resource preparation of glass-containing foams from geopolymers, Ceram. Int. (2019).

[155] H.W. Russell, Principles of heat flow in porous insulators, J. Am. Ceram. Soc. 18 (1935) 1–5.

[156] M. Schmidt, F. Schwertfeger, Applications for silica aerogel products, J. Non. Cryst. Solids. 225 (1998) 364–368.

[157] S. Arcaro, B.G. de O. Maia, M.T. Souza, F.R. Cesconeto, L. Granados, A.P.N. de Oliveira, Thermal Insulating Foams Produced From Glass Waste and Banana Leaves, Mater. Res. 19 (2016) 1064–1069.

[158] Y.N. Qu, W.L. Huo, X.Q. Xi, K. Gan, N. Ma, B.Z. Hou, Z.G. Su, J.L. Yang, High porosity glass foams from waste glass and compound blowing agent, J. Porous Mater. 23 (2016) 1451–1458.

[159] D.U. Tulyaganov, H.R. Fernandes, S. Agathopoulos, J.M.F. Ferreira, Preparation and characterization of high compressive strength foams from sheet glass, J. Porous Mater. 0, (2006) 133–139.

[160] P. Yot, F. Méar, Characterization of lead, barium and strontium leachability from foam glasses elaborated using waste cathode ray-tube glasses, J. Hazard. Mater. 185 (2011) 236–241.

LIST OF PUBLICATIONS

In addition to the first-authoring publications listed in Section 1.3, contribution have been made to the following publications. Moreover, the listed presentations were given at international conferences. It is stated whether the presentation was an oral or a poster contribution.

Publications in peer-reviewed international journals

1. J. König, V. Nemanič, M. Žumer, R.R. Petersen, **M.B. Østergaard**, Y.Z. Yue, and D. Suvorov, "Evaluation of the contributions to the effective thermal conductivity of an open-porous-type foamed glass", *Construction and Building Materials, under review*

2. R.R. Petersen, J. König, N. Iversen, **M.B. Østergaard**, and Y.Z. Yue, "The foaming mechanism of glass foams prepared from Mn_3O_4, carbon and CRT panel glass", *under preparation*

3. M. Stepniewska, **M.B. Østergaard**, C. Zhou, and Y.Z. Yue, "Producing ZIF-62 bulk glasses by optimizing melting process", *under preparation*

Oral and poster presentations at international conferences

4. **M.B. Østergaard**, R.R. Petersen, J. König, H. Johra, and Y.Z. Yue, 100th SGT and ESG 2016, **Oral presentation**, "Influence of foaming agents on both the structure and the thermal conductivity of silicate glasses", Sheffield, United Kingdom, 4-8th September, 2016

5. **M.B. Østergaard**, R.R. Petersen, J. König, M. Bockowski, and Y.Z. Yue, PACRIM 12 including GOMD 2017, **Oral presentation**, "Thermal conductivity of foam glasses prepared using high pressure sintering", Waikoloa, Hawaii, 21-26th May, 2017

6. **M.B. Østergaard**, R.R. Petersen, J. König, M. Bockowski, and Y.Z. Yue, PACRIM 12 including GOMD 2017, **Poster presentation**, "Foaming glass using high pressure sintering", Waikoloa, Hawaii, 21-26th May, 2017

7. **M.B. Østergaard**, B. Cai, R.R. Petersen, J. König, P.D. Lee, and Y.Z. Yue, PNCS - ESG 2018, **Oral presentation**, "Effect of Macrostructure on Thermal Conductivity of Foam Glass", Saint Malo, France, 9-13th July, 2018

8. **M.B. Østergaard**, R.R. Petersen, J. König, and Y.Z. Yue, PNCS - ESG 2018, **Poster presentation**, "Effect of Alkali Phosphate Content on Foaming of CRT Panel Glass Using Mn_3O_4 and Carbon as Foaming Agents", Saint Malo, France, 9-13th July, 2018

ISSN (online): 2446-1636
ISBN (online): 978-87-7210-382-2

AALBORG UNIVERSITY PRESS